Enclosure 2

Structural Integrity Associates Engineering Report No. 0901350.401, Revision 4, "Leak-Before-Break Evaluation – Accumulator, Pressurizer Surge, and Residual Heat Removal Lines, Turkey Point Units 3 and 4," October 12, 2018

Report No.: 0901350.401
Revision No.: 4
Project No.: 1700109
File No.: 0901350.401
October 2018

Leak-Before-Break Evaluation
Accumulator, Pressurizer Surge and Residual Heat Removal Lines
Turkey Point Units 3 and 4

Prepared for:

Florida Power & Light Company
Purchase Order No. 2000230248

Prepared by:

Structural Integrity Associates, Inc.
San Jose, California

Prepared by: Minji Fong — Date: 10/12/2018

Reviewed by: Do Jun Shim — Date: 10/12/2018

Approved by: David A. Gerber — Date: 10/12/2018

REVISION CONTROL SHEET

Document Number: 0901350.401

Title: Leak-Before-Break Evaluation, Accumulator, Pressurizer Surge and Residual Heat Removal Lines, Turkey Point Units 3 and 4

Client: Florida Power & Light Company

SI Project Number: 1700109

Section	Pages	Revision	Date	Comments
Summary 1.0 2.0 3.0 4.0 5.0 6.0 7.0 8.0	iii – x 1-1 – 1-7 2-1 – 2-2 3-1 – 3-3 4-1 – 4-15 5-1 – 5-18 6-1 – 6-13 7-1 – 7-2 8-1 – 8-5	0	4/15/2010	INITIAL ISSUE
3.0 4.0 5.0 6.0 8.0	3-2 4-1, 4-6 5-5, 5-6, 5-13 – 5-19 6-4 8-4	1	5/6/2010	Clients' Comments Addressed
Summary 1.0 6.0 7.0 8.0	v, viii-x 1-1 6-1 – 6-14 7-1 – 7-2 8-4 – 8-5	2	7/10/2017	Updated 60-year results in response to CAR 17-012. Extended evaluation to cover 80 years of operation and to use updated fatigue crack growth law.
Summary 1.0 2.0 3.0 4.0 5.0 6.0 7.0	v 1-1, 1-3 2-1 3-1, 3-2, 3-3 4-2 – 4-5, 4-9, 4-10 5-1 6-2, 6-5, 6-8 – 6-10, 6-13 7-1	3	9/18/2017	Addressed client editorial comments

Summary 5.0 6.0 7.0 8.0	ix 5-3 – 5-23 6-1 – 6-4, 6-6 – 6-12, 6-14 – 6-16, 7-1 – 7-2 8-1, 8-3 – 8-4	4	10/12/2018	Added maximum stress versus critical flaw size plots. Updated through-wall crack growth calculation. Updated references to remove proprietary source.

SUMMARY

This report presents a leak-before-break (LBB) evaluation for the following lines at Turkey Point Nuclear Plant (PTN) Units 3 and 4 operated by Florida Power & Light Company (FPL). These lines are attached to the reactor coolant loop (RCL) and span from the connection to the RCL to the first isolation valve or the pressurizer as applicable:

1. 10" diameter Accumulator Lines – 3 lines (one per RCL connected to cold leg)
2. 12" pressurizer Surge Line – 1 line attached to "B" loop
3. 14" residual heat removal line – 1 line attached to "C" loop in Unit 3 and "A" loop in Unit 4(connected to hot leg)

The evaluation was performed to eliminate consideration of the dynamic effects of the postulated large pipe rupture for these lines. The LBB evaluation was performed in accordance with the 10 CFR 50, Appendix A GDC-4 and NUREG-1061, Vol. 3 [6] as supplemented by NUREG-0800, Standard Review Plan 3.6.3 [7].

The methodology used in determining LBB capabilities of the above lines at PTN Units 3 and 4 consisted of several steps. First, the relationship between the critical through-wall flaw length and the applied stress (or moments) was determined on a generic basis for circumferential flaws. The critical flaw size as used herein refers to the through-wall flaw length that becomes unstable under a given set of applied loads. Critical flaw sizes were calculated using the net limit load (net section plastic collapse) approach with conservative material properties. NUREG-1061[6] requires that the load combination considered in determining the through-wall flaw length include the normal operating loads (NOP), which consists of internal pressure, dead weight, and thermal expansion loads, plus the safe shutdown earthquake (SSE). Once the NOP+SSE load for a given location is known, the critical flaw length can be determined from the generic relationship. The "leakage flaw size" was determined as the minimum of one half the critical flaw size with a factor of unity on normal operating plus SSE loads. Thus, the leakage flaw size

as referred herein maintains a safety factor of 2 on the critical flaw size under normal plus SSE loads.

Leakage rates were determined as a function of stress (or moment) on a generic basis for a given through-wall flaw length. NUREG-1061, Vol. 3 [6] requires that the NOP loads be used to determine the leakage. On a generic basis, a family of curves was developed relating the leakage with the NOP loads to the through-wall flaw length.

Given the relationships between the leakage flaw size versus NOP+SSE moments and leakage flaw size versus NOP moments above (for a particular leak rate), a relationship was developed between the NOP+SSE moments and the NOP moments that would result in a particular leak rate. This results in the bounding analysis curve (BAC). The actual piping NOP+SSE and NOP loads were then used to determine if the combination of those loads would meet that leakage (fall below the BAC). This particular scheme is very convenient for determining whether or not a particular leakage will be met for a piping system with many nodal points and associated moments, such as the auxiliary RCL piping lines considered in this evaluation.

A fatigue crack growth analysis was also performed to determine the growth of postulated semi-elliptical, inside surface flaws with an initial size based on ASME Code, Section XI [26] acceptance standards. This showed that crack growth due to cyclic loadings was not significant such that it could be managed by the Section XI inspection program. In addition, a fatigue crack growth analysis was performed to show that a through-wall crack would not grow significantly, hereby, insuring that the leakage size flaw will not grow to the critical crack size.

The following summary of the LBB evaluation is formatted along the lines of the "Recommendations for Application of the LBB Approach" in the NUREG-1061 Vol. 3 [6] executive summary:

(a) The three piping systems considered in this evaluation are constructed of A 376 Type 316 stainless steel piping. At the operating temperature of these piping lines of 550°F to 653°F, this material is very ductile and it is not susceptible to cleavage-type fracture. In addition, these systems have been shown not to be susceptible to the effects of corrosion, high cycle fatigue or water hammer.

(b) Loadings have been determined from the original piping analysis, and are based upon pressure, dead weight, thermal expansion, and safe shutdown earthquake. All stress locations in these piping systems from the connection to the RCL to the first isolation valve or pressurizer, as applicable, were considered.

(c) Minimum ASME Code material properties were used to establish conservative lower bound stress-strain properties to be used in the evaluations. For the fracture toughness properties, lower-bound generic industry material properties for the piping and welds have been conservatively used in the evaluations.

(d) Crack growth analysis was conducted at the most critical locations on the evaluated piping, considering the cyclic stresses predicted to occur over the life of the plant. For a hypothetical flaw with aspect ratio of 10:1 and an initial flaw depth of 12.5% of pipe wall, the final flaw size after considering all plant transients for both 60 years and 80 years of operation is less than ASME Code Section XI allowable flaw size of 75%. Hence, fatigue crack growth is well within the allowable flaw size for the auxiliary RCL piping.

(e) The LBB evaluation is performed for leakage rates of 2 GPM (gallons per minute), 5 GPM and 10 GPM. All piping locations considered in the evaluation exhibit a minimum leakage rate of 10 GPM based on the normal operating and normal plus dynamic loads. NUREG-1061 Vol. 3 recommends that the leakage detection system be capable of measuring leakage rates 1/10 of the minimum leakage rate. The plant leak detection capability for both Units 3 and 4 is 1 GPM [8], thereby satisfying the leakage rate requirement.

(f) Each of the piping systems considered in this evaluation is less than 51.2 feet in length and is not geometrically complex.

(g) Crack growth of a leakage size crack due to a conservative seismic event was insignificant and the final crack size was smaller than the critical crack size.

(h) For all locations, the critical size circumferential crack was determined for the combination of absolute values of normal operating plus SSE loads. The leakage size flaw was chosen such that its length was no greater than the critical crack size reduced by a factor of two for conservatism. Axial cracks were not considered as they are known to exhibit much higher leakage and more margin than circumferentially oriented cracks.

(i) Another LBB acceptance criterion is, for all locations, determine the critical crack size for the combination of 1.4 times the normal plus SSE loads and select the leakage crack no greater than this critical crack size. Based on previous experience, this criterion is always bounded by the criterion of (h) above. Hence, in this evaluation, only the evolution based on criterion of (h) is performed.

(j-n) No special testing was conducted to determine material properties for fracture mechanics evaluation. Instead, ASME Code minimum properties were utilized in the evaluations. The material properties so determined have been shown to be applicable near the upper range of normal plant operation and exhibit ductile behavior at these temperatures.

(o) Limit load analysis as outlined in NUREG-0800, SRP 3.6.3, was utilized in this evaluation in order to determine the critical flaw sizes since the materials involved in this evaluation are stainless steel piping.

Thus, the three piping systems evaluated in this report for PTN Units 3 and 4 qualify for the application of leak-before-break analysis to demonstrate that it is very unlikely that the piping could experience a large pipe break prior to leakage detection. Results of the evaluation show that for all applicable pipe stresses, leak-before-break can be justified for a plant leak detection system of 1 GPM.

Table of Contents

List of Tables

List of Figures

1.0 INTRODUCTION

1.1 Background

In 2009, Florida Power & Light Company (FPL) embarked on an Extended Power Uprate (EPU) project at Turkey Point Nuclear Plant (PTN) Units 3 and 4. Prior to EPU implementation, each of the PTN units was licensed to a core power rating of 2300 MWth. The EPU resulted in a new core power rating of 2644 MWth at PTN, which includes a 1.7% Measurement Uncertainty Recapture (MUR) [1]. Reactor coolant loop (RCL) pipe break design basis scenarios generally produce large hydrodynamic loads that must be considered in the design of plant safety systems. At PTN, the leak-before-break (LBB) methodology was applied to the primary RCL piping and approved by the US Nuclear Regulatory Commission (NRC). Branch lines connected to the RCL also benefit from the use of LBB methodology, which eliminates from the plant design basis the consideration of those auxiliary pipe break loads.

This report documents evaluations performed by Structural Integrity Associates (SIA) to determine LBB capabilities of the high energy, non-isolable, auxiliary piping attached to the RCL at PTN Units 3 and 4. In this revision of the report, the previous fatigue crack growth evaluation for 60 years is updated to use the current version of the **pc-CRACK** software (**pc-CRACK 4.1** [49a]) and to correct for the errors documented in Corrective Action Report (CAR) 17-012 [54]. The new fatigue crack growth results are shown in Table 6-10. Also, fatigue crack growth for 80 years of operation is added to address Subsequent License Renewal (SLR) operation utilizing the updated ASME Code Case N-809 [53] fatigue crack growth rate.

The following lines at PTN Units 3 and 4 are considered in this evaluation.

1. 10" diameter Accumulator Lines – 3 lines (one per RCL connected to cold leg)
2. 12" pressurizer Surge Line – 1 line attached to "B" loop
3. 14" residual heat removal line – 1 line attached to "C" loop in Unit 3 and "A" loop in Unit 4 (connected to hot leg)

The approach taken to address LBB for the lines at PTN delineated above is consistent with that used by SI in recent LBB submittals for other plants [2, 3, 4].

1.2 Leak-Before-Break Methodology

NRC SECY-87-213 [5] covers a rule to modify General Design Criterion 4 (GDC-4) of Appendix A, 10 CFR Part 50. This amendment to GDC-4 allows exclusion from the design basis of all dynamic effects associated with high energy pipe rupture by application of LBB technology.

Definition of the LBB approach and criteria for its use are provided in NUREG-1061 [6], supplemented by NUREG-0800, SRP 3.6.3 [7]. Volume 3 of NUREG-1061 defines LBB as "...the application of fracture mechanics technology to demonstrate that high energy fluid piping is very unlikely to experience double-ended ruptures or their equivalent as longitudinal or diagonal splits." The particular crack types of interest include circumferential through-wall cracks (TWC) and part-through-wall cracks (PTWC), as well as axial or longitudinal through-wall cracks (TWC), as shown in Figure 1-1.

LBB is based on a combination of in-service inspection (ISI) and leak detection to detect cracks, coupled with fracture mechanics analysis to show that pipe rupture will not occur for cracks smaller than those detectable by these methods. A discussion of the criteria for application of LBB is presented in Section 2 of this report, which summarizes NUREG-1061, Vol. 3 requirements.

The approach to LBB which has gained acceptance for demonstrating protection against high energy line break (HELB) in safety-related nuclear piping systems is schematically illustrated in Figure 1-2. Essential elements of this technique include critical flaw size evaluation, crack propagation analysis, volumetric nondestructive examination (NDE) for flaw detection/sizing, leak detection, and service experience. In Figure 1-2, a limiting circumferential crack is modeled as having both a short through-wall component, or an axisymmetric part-through-wall crack component. Leak detection establishes an upper bound for the through-wall crack component while volumetric ISI limits the size of undetected part-through-wall defects. These detection methods complement each other, since volumetric NDE techniques are well suited to the detection of long cracks while leakage monitoring is effective in detecting short through-wall cracks. The level of NDE required to support LBB involves volumetric inspection at intervals determined by fracture mechanics crack growth analysis, which would preclude the growth of detectable part-through-wall cracks to a critical size during an inspection interval. A fatigue evaluation is performed to ensure that an undetected flaw acceptable per ASME Section will not grow significantly during service. For through-wall defects, crack opening areas and resultant leak rates are compared with leak detection limits.

The net effect of complementary leak detection and ISI is illustrated by the shaded region of Figure 1-2 as the largest undetected defect that can exist in the piping at any given time. Critical flaw size evaluation, based on elastic-plastic fracture mechanics techniques, is used to determine the length and depth of defects that would be predicted to cause pipe rupture under specific design basis loading conditions, including abnormal conditions such as a seismic event and including appropriate safety margins for each loading condition. Crack propagation analysis is used to determine the time interval in which the largest undetected crack could grow to a size which would impact plant safety margins. A summary of the elements for a leak-before-break analysis is shown in Figure 1-3. Service experience, where available, is useful to confirm analytical predictions as well as to verify that such cracking tends to develop into "leak" as opposed to "break" geometries.

In accordance with NUREG-1061, Vol. 3 [6] and NUREG-0800, SRP 3.6.3 [7], the leak-before-break technique for the high energy piping systems evaluated in this report included the following considerations.

- Elastic-plastic fracture mechanics analysis of load carrying capacity of cracked pipes under worst case normal loading, with safe-shutdown earthquake (SSE) and other dynamic loads included. Such analysis includes elastic-plastic fracture data applicable to pipe weldments and weld heat affected zones where appropriate. In this evaluation, elastic-plastic fracture mechanics (EPFM) was not applied.

- Limit-load analysis in lieu of the elastic-plastic fracture mechanics analysis described above can be used to determine critical flaw sizes. Because the material for all the piping systems considered in this evaluation is stainless steel, limit load analysis was used.

- Linear elastic fracture mechanics analysis of subcritical crack propagation to determine ISI (in-service inspection) intervals for long, part-through-wall cracks.

Piping stresses have a dual role in LBB evaluations. On one hand, higher maximum (design basis) stresses tend to yield lower critical flaw sizes, which result in smaller flaw sizes for assessing leakage. On the other hand, higher operating stresses tend to open cracks more for a given crack size and create a higher leakage rate. Because of this duality, the use of a single maximum stress location for a piping system may result in a non-conservative LBB evaluation. Thus, the LBB evaluation reported herein has been performed for each nodal location addressed in the plant piping system analysis for the affected portions.

1.3 Leak Detection Requirement

Application of LBB evaluation methodology is predicated on having a very reliable leak detection system at the plant. This evaluation will determine the minimum leakage rate based on the normal operating and normal plus dynamic loads for the five auxiliary RCL piping lines in each Units 3 and 4. NUREG-1061 requires the demonstration of leak detection capability of leak rates of 1/10 of this amount. Per reference 8, the leak detection system at PTN is capable of detecting 1 GPM.

FPL is committed to US Nuclear Regulatory Commission (NRC) Generic Letter (GL) 84-04 [52] which considers a four hour response time for detecting 1 GPM leak rate.

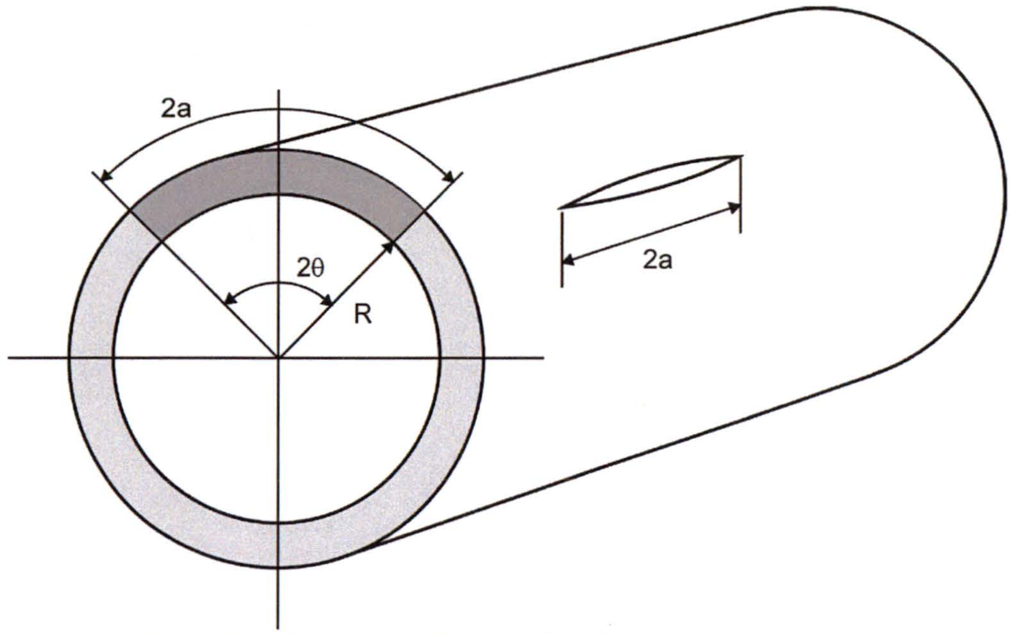

a. Circumferential and Longitudinal Through-Wall Cracks of Length 2a.

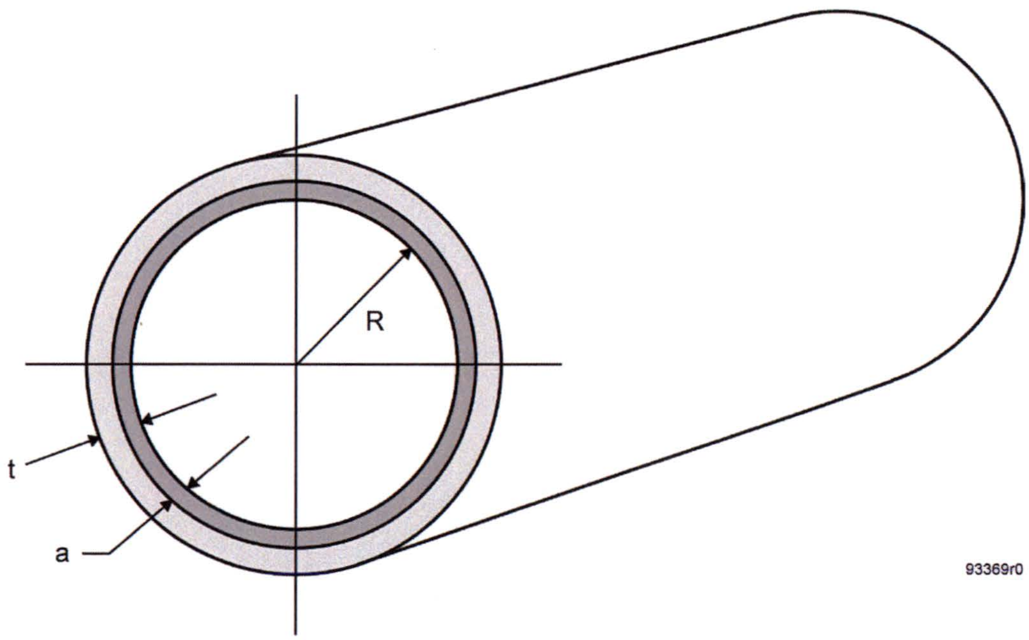

b. Circumferential 360 Part-Through-Wall Crack of Depth a.

Figure 1-1. Representation of Postulated Cracks in Pipes for Fracture Mechanics Leak-Before-Break Analysis

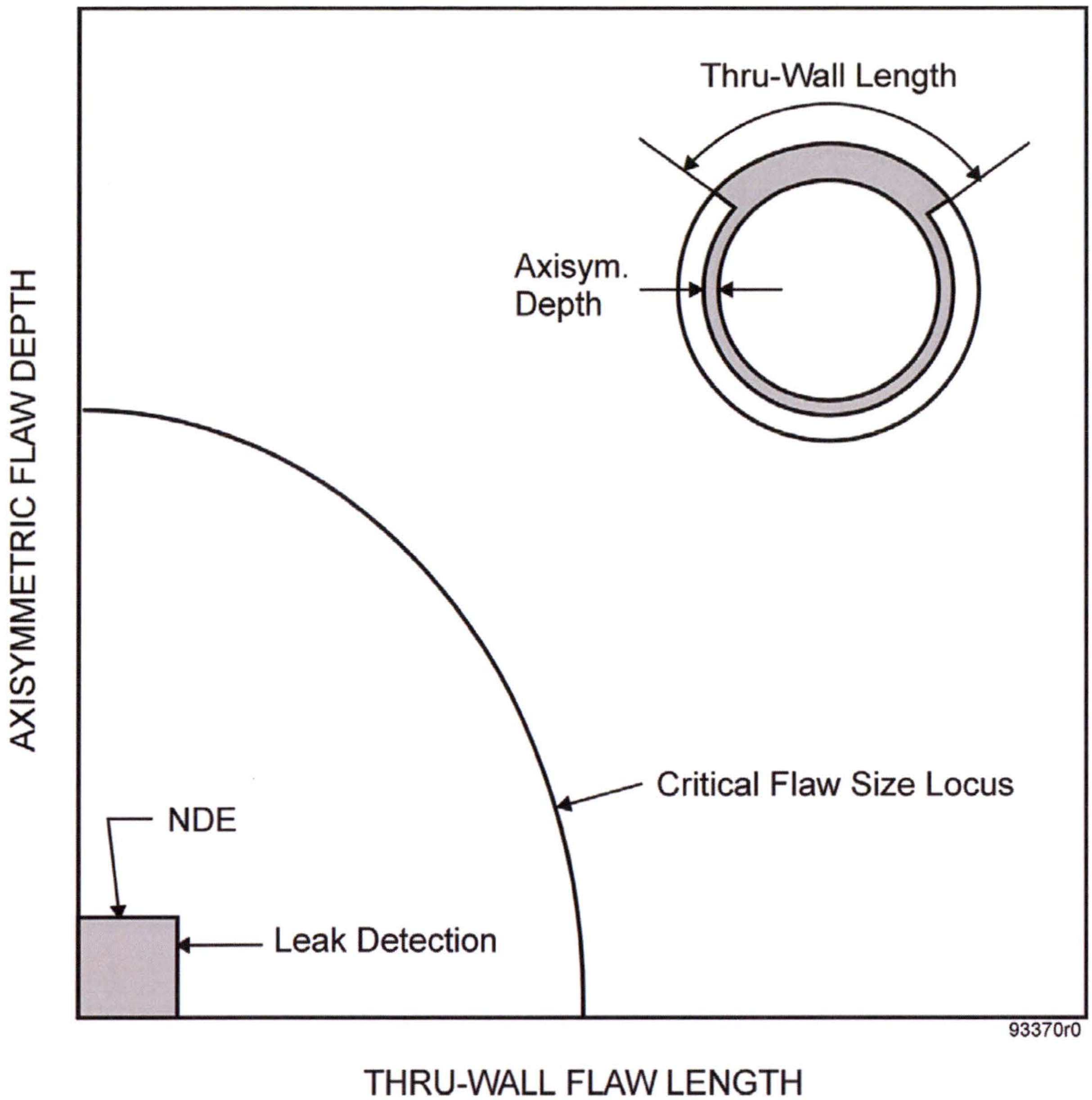

Figure 1-2. Conceptual Illustration of ISI (UT)/Leak Detection Approach to Protection Against Pipe Rupture

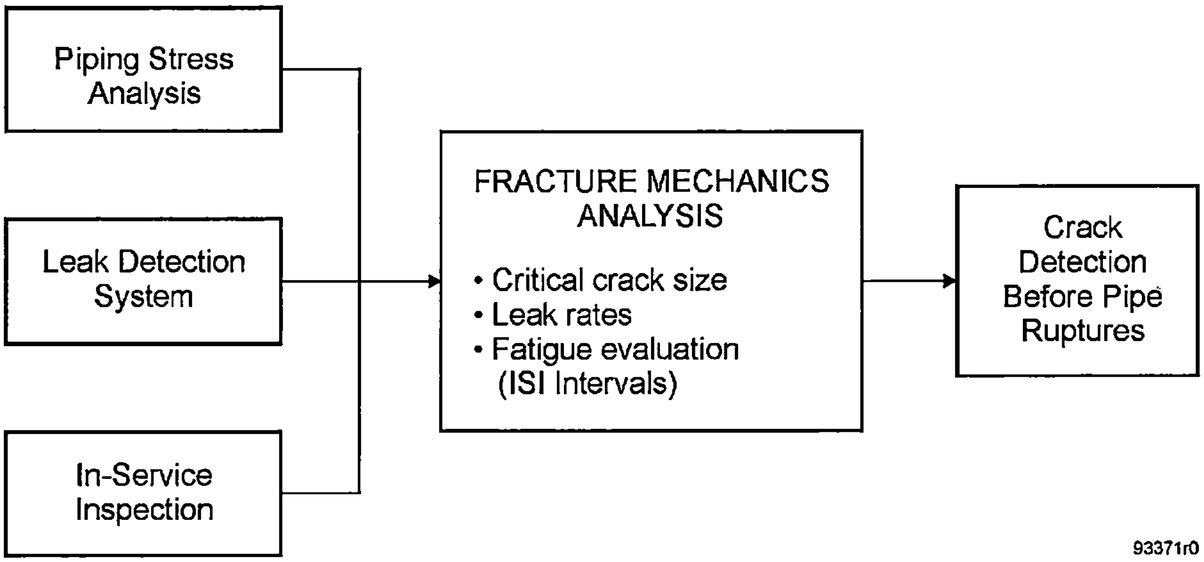

Figure 1-3. Leak-Before-Break Approach Based on Fracture Mechanics Analysis with In-service Inspection and Leak Detection

2.0 CRITERIA FOR APPLICATION OF LEAK-BEFORE-BREAK

NUREG-1061, Vol. 3 [6] identifies several criteria to be considered in determining applicability of the leak-before-break approach to piping systems. Section 5.2 of NUREG-1061, Vol. 3 provides extensive discussions of the criteria for performing leak-before-break analyses. These requirements are restated in NUREG-0800, SRP 3.6.3 [7]. The details of the discussions are not repeated here; the following summarizes the key elements:

2.1 Criteria for Through-Wall Flaws

Acceptance criteria for critical flaws may be stated as follows:

1. A critical flaw size shall be determined for normal operating conditions plus safe shutdown earthquake (SSE) loads. Leakage for normal operating conditions must be detectable for this flaw size reduced by a factor of two.

2. A critical flaw size shall be determined for normal operating conditions plus SSE loads multiplied by a factor of $\sqrt{2}$. Leakage for normal operating conditions must be detectable for this flaw size.

Previous evaluations conducted by Structural Integrity Associates (SIA) have found through experience from previous LBB analyses that the first criterion bounds the second. Hence, in this evaluation, only the first criterion was considered. Previous evaluations have found that the critical through-wall flaw length for an axial flaw is always greater than that of a circumferential flaw. Also, the higher hoop stress results in more leakage for an axial flaw compared to a circumferential flaw of the same length. Since axial flaws have both a larger critical through wall flaw length and more leakage for a given flaw size compared to circumferential flaws, only circumferential flaws are considered in this evaluation.

Either elastic-plastic fracture mechanics instability analysis or limit load analysis may be used in determining critical flaw sizes. Since the material of the piping systems considered at PTN is stainless steel, which is ductile at high temperatures, the limit load methodology is used in this evaluation to determine the critical flaw sizes.

2.2 Criteria for Part-Through-Wall Flaws

NUREG-1061, Vol. 3 [6] requires demonstration that a long part-through-wall flaw which is detectable by ultrasonic means will not grow due to fatigue to a depth which would produce instability over the life of the plant. This is demonstrated in Section 6.0 of this report, where the analysis of subcritical crack growth is discussed.

2.3 Consideration of Other Mechanisms

NUREG-1061, Vol. 3 [6] limits applicability of the leak-before-break approach to those locations where degradation or failure by mechanisms such as water hammer, erosion/corrosion, fatigue, and intergranular stress corrosion cracking (IGSCC) is not a significant possibility. These mechanisms were considered for the auxiliary RCL piping at PTN Units 3 and 4, as reported in Section 3 of this report.

3.0 CONSIDERATION OF WATER HAMMER, CORROSION AND FATIGUE

NUREG-1061, Vol. 3 [6] states that LBB should not be applied to high energy lines susceptible to failure from the effects of water hammer, corrosion or fatigue. These potential failure mechanisms are thus discussed below with regard to the affected RCL piping at PTN Units 3 and 4, and the above failure mechanisms are determined not to invalidate the use of LBB for this piping.

3.1 Water Hammer

A comprehensive study performed in NUREG-0927 [9] indicated that the probability of water hammer occurrence in the residual heat removal systems of a pressurized water reactor (PWR) is very low. In NUREG-0927, only a single event of water hammer was reported for PWR residual heat removal systems with the cause being incorrect valve alignment. There was no indication as to which portion of the system was affected but it would not be that portion adjacent to the reactor coolant system (RCS) attached piping evaluated for LBB.

NUREG-0927 also reported that the safety significance of water hammer events in the safety injection system is moderate. With four water hammer events reported in the safety injection systems, three of these events were associated with voided lines and the other event was associated with steam bubble collapse. Although there was no indication of the affected portions of the safety injection system, the portions susceptible to water hammer would not be that adjacent to the RCS-attached piping evaluated for LBB.

The portions of the piping evaluated for LBB are inboard of the first isolation valves for the safety injection (accumulator) and residual heat removal (RHR) piping. Thus, during normal operation, these lines experience reactor coolant pressure and temperature conditions such that there is no potential for steam/water mixtures that might lead to water hammer. The portions of these systems that are adjacent to the reactor coolant piping are not in use during normal operation. The RHR system is not used except during low-pressure low-temperature cooldown conditions. The safety injection system is used only during loss of coolant-accident (LOCA) conditions. During normal plant operation, the portions of the system beyond the first isolation valve are expected to run at low temperature conditions. Thus, there should never be any voiding or potential for steam bubble collapse, which could result in water hammer loads on the piping attached directly to the RCS considered in this evaluation. To date, there has been no experience related to water hammer events in either the RHR or safety injection systems at PTN.

Per Reference 52, a search of FPL's condition report databases was performed to verify if water hammer events have occurred on the RHR Lines being analyzed for LBB evaluation. The search looked back as early as 1992 for past events of water hammer in RHR Lines and none were found in the Condition Reports Databases of PTN, Units 3 and 4. Therefore, water hammer is highly unlikely for the piping systems under consideration in this report. Hence, this phenomenon will have no impact on the LBB analysis for the affected portions of the safety injection and residual heat removal systems at PTN.

The surge line also experiences reactor coolant pressure and temperature conditions such that there is no potential for steam/water mixtures that might lead to water hammer.

3.2 Corrosion

Two corrosion damage mechanisms which can lead to rapid piping failure are intergranular stress corrosion cracking (IGSCC) in austenitic stainless steel pipes and flow-assisted corrosion (FAC) in carbon steel pipes. IGSCC has principally been an issue in austenitic stainless steel piping in boiling water reactors [10] resulting from a combination of tensile stresses, susceptible material and oxygenated environment. IGSCC is not typically a problem for the primary loop of a PWR fabricated from stainless steel such as the SI accumulator, Surge Line and RHR systems under consideration since the environment has relatively low concentrations of oxygen. There are no Alloy 600/82/182 materials in the 5 auxiliary lines evaluated in this report. Hence, PWSCC (IGSCC in primary water environment of PWRs) is not an active degradation mechanism.

FAC is a problem for carbon steel piping with two-phase flow [11]. FAC is not anticipated t for the systems under consideration in this report since the piping is fabricated from stainless steel which is not susceptible to FAC.

3.3 High Cycle Fatigue

Metal fatigue in piping systems connected to the reactor coolant loops of Westinghouse-designed pressurized water reactor was identified in Bulletin 88-08 [12]. Evaluations performed by FPL and submitted to the Nuclear Regulatory Commission have concluded that the bulletin does not apply to PTN [52]. For the SI accumulator piping, there is no interconnection to the charging pumps that will lead to inleakage leading to cracking such was identified at Farley and Tihange. For the RHR piping, any outleakage at the isolation valve leak off lines is monitored and can be corrected such that cracking similar to that identified at the Japanese Genkai plant will not occur. Thus, there is no potential for unidentified high cycle fatigue.

Known fatigue loadings and the resultant possible crack growth have been considered by the analyses reported in Section 6.0 of this report. Based on the results presented in Section 6.0, it is concluded that fatigue will not be a significant issue for the piping systems under consideration at PTN Units 3 and 4.

4.0 PIPING MATERIALS AND STRESSES

4.1 Piping System Description, Operating Conditions and Geometry

The piping systems considered in this evaluation have been described in Section 1.1. Schematics of these lines including selected nodal points are shown in Figures 4-1 through 4-6.

4.1.1 Accumulator Lines

The normal operating temperature and pressure for the 10" Accumulator Lines are 555 °F and 2485 psig for all the three RCLs (A, B, and C) in both units 3 and 4 [13, 14].

Per Reference 14 for Unit 4 Accumulator Lines, per Reference 44(a) for Unit 3 Accumulator Lines, and per the standard piping schedule [15] for Unit 3 Accumulator Lines, the pipe outer diameter (OD) is 10.75" and the pipe thickness is 1".

4.1.2 Pressurizer Surge Line

The normal operating temperature and pressure for the 12" pressurizer Surge Line are 653 °F and 2235 psig (RCL B only) in both units 3 and 4 for the pressurizer end [16]. For the hot leg end, the normal operating temperatures and pressure are 602.1/602.3/610.9 °F and 2235 psig (RCL B only) in both units 3 and 4 [17, 18]. The different temperatures at the hot leg end come from different specification documents as listed in References 17 and 18. For critical flaw size calculations, a higher temperature gives lower material properties (less plastic moment) and hence is conservative. For leakage calculations a lower temperature gives higher material properties (less crack opening) and hence is conservative. Therefore, at the hot leg end of the pressurizer Surge Line, a temperature of 602.1 °F will be considered for leakage and a temperature of 610.9 °F will be considered for critical flaw size evaluation.

Per Reference 16, the nominal pipe OD of the pressurizer Surge Line is 12" and it is a schedule 140 pipe made of stainless steel material for both Units 3 and 4. Therefore, from the standard piping schedule [15] the pipe outer diameter (OD) is 12.75" and the pipe thickness is 1.125".

From References 38, 43 and 16, a 14" to 12" reducer is present at the pressurizer Surge Line nozzle. Per Reference 46, the Surge Line pipe OD is 14" + 4* Tan (10°) = 15.41" and the thickness is 1.765" at the centerline of the pressurizer nozzle. Since the thermal sleeve starts from the nozzle weld it will be conservatively considered for the leakage purpose as it increases the flow path length. Per Reference 46 the thermal sleeve thickness is 0.19". Since a similar 14" to 12" reducer is used at the hot leg end [38, 43] also, the same pipe geometry will be used.

4.1.3 RHR Line

The normal operating temperatures and pressure for the 14" RHR Line are 602.1/602.3/610.9 °F and 2235 psig (RCL C for Unit 3 and RCL A for Unit 4) in both units 3 and 4 for the hot leg end [17, 18].

Therefore, for leakage evaluation a hot leg temperature of 602.1 °F will be considered. For critical flaw size evaluation, a hot leg temperature of 610.9 °F will be considered.

Per References 19 and 47 the pipe OD is 14" and the pipe thickness is 1.25".

A summary of the operating conditions for the five lines are presented in Tables 4-1 and 4-2 for leakage and critical flaw size calculations, respectively. A summary of the pipe geometry for these lines is provided in Tables 4-3 and 4-4 for leakage and critical flaw size calculations, respectively.

4.2 Material Properties

From the material specification documents [21], the base material used for all the piping systems with diameters between 10" and 16" is SA 376 Type 316 (corresponds to ASME designation of A 376). From Reference 22, the welding procedure is either gas tungsten arc weld (GTAW) or shielded metal arc weld (SMAW) except for the nozzle welds which are TIG (tungsten inert gas) welds [23]. Since SMAW weld has a lower toughness (i.e., higher Z factor per ASME Section XI, IWB-3640 rules) than GTAW/TIG welds, it is assumed conservatively to be the only weld process used for all the cases. Per Reference 24, the weld material used is Type 316/317/317L. A Type 317L material is conservatively used for the flaw size calculation as it provides lower yield strength compared to that of the base material A 376 Type 316, which is conservatively used for the leakage evaluation. Similarly, A 376 Type 316 material gives lower Ramberg-Osgood parameters compared to Type 317L material and are therefore, is used for the leakage calculation.

The material properties per ASME Code Section II, Part D [25] are summarized in Tables 4-5 and 4-7 for the leakage evaluation and in Table 4-6 for the critical flaw size evaluation.

4.2.1 Calculation of Z Factors for Fracture Mechanics Analysis

The pressurizer surge, the accumulator, and the RHR Lines are made of austenitic stainless steel weld materials. Per ASME Code, Section XI, Appendix C [26], Section C-6330, the Z factor of austenitic stainless steel weld materials fabricated using the SMAW process is calculated as follows:

$Z = 1.30[1+0.010(NPS-4)]$ for submerged arc weld (SAW) (used conservatively since Z factor for SAW is higher than for SMAW)

where:

NPS = nominal pipe size, in; NPS is taken as the outside diameter (OD) of the component.

Z factors for the weld material used in the flaw size calculation are shown in Table 4-6. Since wrought stainless steel (A 376 Type 316) is used for the pipe material (elbow and straight sections), a Z factor of 1.0 can be applied.

4.2.2 Determination of Ramberg-Osgood Material Parameters

For the leakage calculation, the Ramberg-Osgood material parameters are required. The Ramberg-Osgood stress-strain parameters used to describe the true stress-strain curve were obtained from the mechanical properties using the correlations developed in Reference 27. The true stress-true strain curve can be represented by the following relationship:

$$\frac{\varepsilon}{\varepsilon_0} = \frac{\sigma}{\sigma_0} + \alpha\left(\frac{\sigma}{\sigma_0}\right)^n \tag{4-1}$$

where: ε, σ are the true strain and true stress,

ε_o, σ_o are the yield strain and yield stress, and

α, n are the Ramberg-Osgood parameters.

The values of α and n are then obtained from the relationship provided in Reference 27 as:

$$n = \frac{1}{\ln(1+e_u)} \tag{4-2}$$

$$\alpha = \left[\frac{\ln(1+e_u)}{\ln\left(1+\frac{S_y}{E}\right)} - \frac{S_u(1+e_u)}{S_y\left(1+\frac{S_y}{E}\right)}\right]\left[\frac{S_u(1+e_u)}{S_y\left(1+\frac{S_y}{E}\right)}\right]^{-n} \tag{4-3}$$

where, e_u is the ultimate elongation, S_y/S_u is yield/ultimate strength, and E is the elastic modulus.

All the stress-strain properties used in this evaluation are provided in Table 4-7.

4.3 Applicable Stresses

The piping moments and stresses considered in the LBB evaluation are due to pressure (P), dead weight (DW), thermal expansion (TE), thermal stratification (STRAT, if present), safe shutdown earthquake inertia (SSE) and seismic anchor movements (SAM) consistent with the guidance provided in NUREG-1061, Vol. 3. Per the guidance provided in NUREG-1061, other secondary stresses such as residual stresses and through-wall thermal stresses were not included in the evaluation.

For calculation of leakage, the normal operating (NOP) loads consisting of pressure, dead weight and thermal expansion loads are used. For calculation of critical flaw size, the maximum of

STRAT and SSE with SAM loads is added to the NOP loads (referred to as the NOP + SSE loading condition).

The applicable loads to be used in conjunction with the bounding analysis curves (BAC) developed based on plant operating conditions, pipe geometry, material properties are reported in Tables 4-8 through 4-13 [16, 44, 45, 46, 47, 48].

The axial stress due to normal operating pressure is calculated from the expression:

$$\sigma_p = \frac{pD_i^2}{D_o^2 - D_i^2}$$

where p is the internal pressure, D_o is the outside diameter of the pipe and D_i is the inside diameter.

The bending stress due to dead weight, thermal expansion and SSE is calculated from the bending moments using the expression:

$$\sigma_m = \frac{M_r}{Z}$$

where:

Z	=	the section modulus and,
M_r	=	the resultant moment.

Axial forces due to dead weight, thermal expansion, seismic, were not considered in the evaluation. The stresses due to axial forces are not significant compared to those from pressure loads, so their exclusion does not significantly affect the results of this evaluation. This has been shown in a previous LBB submittal [4].

Table 4-1. Normal Operating Conditions for Leakage Evaluation

Parameter	Accumulator Line	Surge Line		R H R Line
	Cold Leg End	Pressurizer End	Hot Leg End	Hot Leg End
Temperature, °F	555[1]	653[2]	602.1[2]	602.1[3]
Pressure, psig	2485[1]	2235[2]		2235[3]

Notes:

1. Normal operating temperature and pressure for all three RCLs A, B, and C in both Units 3 and 4.
2. Normal operating temperature and pressure for RCL B only in both Units 3 and 4.
3. Normal operating temperatures and pressure for RCL C and RCL A in Units 3 and 4, respectively, for the hot leg.

Table 4-2. Operating Conditions for Critical Flaw Size Evaluation

Parameter	Accumulator Line	Surge Line		R H R Line
	Cold Leg End	Pressurizer End	Hot Leg End	Hot Leg End
Temperature, °F	555[1]	653[2]	610.9[2]	610.9[3]
Pressure, psig	2485[1]	2235[2]		2235[3]

Notes:

1. Normal operating temperature and pressure for all three RCLs A, B, and C in both Units 3 and 4.
2. Normal operating temperature and pressure for RCL B only in both Units 3 and 4.
3. Normal operating temperatures and pressure for RCL C and RCL A in Units 3 and 4, respectively, for the hot leg.

Table 4-3. Pipe Geometry Inputs for Leakage Evaluation

	Accumulator Line	Surge Line		R H R Line
		Pipe Side	Nozzle Side	
Outside Diameter, in	10.75	12.75	15.41	14.00
Thickness, in	1.00	1.125	1.955[1], [2]	1.25

Note:

1) For the leakage evaluation, as explained in Section 4.1.2, the thickness of the Surge Line at the nozzle side (1.955 in) includes the thickness of the thermal sleeve (0.19 in) and that of the nozzle side (1.955 in = 1.765 in + 0.19 in).
2) Used for nozzle sides at hot leg end and the pressurizer end.

Table 4-4. Pipe Geometry Inputs for Critical Flaw Size Evaluation

	Accumulator Line	Surge Line		RHR Line
		Pipe Side	Nozzle Side	
O. D., in	10.75	12.75	15.41	14.00
Thickness, in	1.00	1.125	1.765	1.25

Table 4-5. ASME Code Strength at Normal Operating Temperatures for Leakage Calculation

Components	Material Designation	Leakage			
		S_y (ksi)	S_u (ksi)	σ_{flow} (ksi) (1)	E (ksi)
Surge Line at Hot Leg (602.1°F)	A-376 TP316	18.88	71.80	45.34	25289.5
Surge Line at Pressurizer (653°F)	A-376 TP316	18.48	71.80	45.14	25035.0
RHR Line at Hot Leg (602.1°F)	A-376 TP316	18.88	71.80	45.34	25289.5
Accumulator Line (546.2°F) (2)	A-376 TP316	20.00	71.80	45.90	25569.0

Note:

1) Per Reference 7, the flow stress (σ_{flow}) is the average of the ultimate strength, S_u, and the yield strength, S_y at normal operating temperature [$\sigma_{flow} = 0.5(S_u + S_y)$].
2) Conservatively assumed cold leg normal operating temperature [17, 18] which is less than 555°F.

Table 4-6. ASME Code Strength at Normal Operating Temperatures for Critical Flaw Size Calculation

Components	Material Designation	S_y (ksi)	S_u (ksi)	σ_{flow} (ksi) (1)	Z factor
Surge Line at Hot Leg (610.9°F)	Type 317L (SA-240(2))	18.61	66.10	42.36	1.466(3), 1.500(4)
Surge Line at Pressurizer (653°F)	Type 317L (SA-240(2))	18.28	66.09	42.19	1.466(3), 1.500(4)
RHR Line at Hot Leg (610.9°F)	Type 317L (SA-240(2))	18.61	66.10	42.36	1.482
Accumulator Line at Cold Leg (555°F)	Type 317L (SA-240(2))	19.15	66.15	42.65	1.444

Note:
1. Per Reference 7, the flow stress (σflow) is the average of the ultimate strength, Su, and the yield strength, Sy at normal operating temperature [σflow =0.5(Su + Sy)].
2. SA-240 assumed for conservatism.
3. Pipe side.
4. Nozzle side.

Table 4-7. Ramberg-Osgood Parameters for Leakage Calculation

	Ramberg Osgood Parameter α	Ramberg Osgood Exponent n
Surge Line at Hot Leg (602.1°F)	2.679	2.988
Surge Line at Pressurizer (653°F)	2.709	2.946
RHR Line at Hot Leg (602.1°F)	2.679	2.988
RHR Line at Cold Leg (546.2°F)	3.557	3.104
Accumulator Line (555°F)	2.567	3.093

Table 4-8. Load Points for Accumulator Lines

Unit 3		
NODE POINTS	NOP (ksi)	MAX (ksi)
460	6.3595407	13.13421
460	6.3595407	13.13421
470 B	5.0286469	8.0064046
470 B	5.0286469	12.026137
470 M	5.8448435	9.6070015
470 M	5.8448435	9.6070015
470 E	6.5103769	11.547761
470 E	6.510492	11.585303
475 B	6.5287801	11.628064
475 B	6.5288367	11.58679
475 M	7.7986352	14.739055
475 M	7.7986352	14.739055
475 E	8.641909	18.087145
475 E	8.6420909	18.540287
480	8.7326104	19.024855
610	4.9364849	7.148956
610	4.9364849	7.148956
615	5.2555545	8.4411515
615	5.2555545	8.4411515
625 B	5.2546522	8.3181221
625 B	5.2546522	8.3181997
625 M	5.271894	8.0773594
625 M	5.271894	8.0773594
625 E	5.3389725	7.8955707
625 E	5.3389725	7.8957902
630 B	5.4250361	8.015566
630 B	5.4250596	8.0155966
630 M	5.5590757	8.5960804
630 M	5.5590757	8.5960804
635 B	5.7404138	8.4769993
635 B	5.7405555	8.62194
635 M	5.9553124	9.2302237
635 M	5.9553124	9.2302237
636	6.1454537	10.271527
636	6.1456297	10.271453
637	6.1969734	10.603023

Unit 4		
NODE POINTS	NOP (ksi)	MAX (ksi)
110	5.8290139	11.465209
110	5.8290433	11.465263
120 B	6.8707021	12.531389
120 B	6.8705541	12.531548
120 M	7.4736314	14.131029
120 M	7.4736314	14.131029
120 E	7.5070712	14.804157
120 E	7.5076533	15.210674
122 B	7.5073396	15.210887
122 B	7.5073191	14.865775
122 M	7.656345	16.240519
122 M	7.656345	16.240519
124	8.5255197	18.173109
124	8.5255633	18.172721
200 B	5.4518614	9.3544977
200 E	5.4518091	9.3544479
204	5.4834917	7.9301628
204	5.3945135	7.9300164
206 B	5.4733183	7.7320302
206 B	5.396645	7.7320562
206 M	5.3413536	7.4375186
206 M	5.6637209	7.2925118
206 E	5.5640694	7.5952068
206 E	5.5640694	8.77403
208 B	6.0785518	8.8644482
208 B	6.0785518	11.00678
208 B	7.0049967	11.185453
208 B	7.0024718	12.956097
208 E	7.4932366	13.128829
208 E	7.4931974	13.072252
210 B	7.4864591	13.207919
210 B	7.494673	16.124818
210 M	8.06121	16.031819
210 M	8.06121	18.616902
210 E	8.6170688	18.752244
210 E	8.6169865	18.878764

Table 4-8 Load Points for Accumulator Lines (Continued)

637	6.1969936	10.64815
638	6.2180447	10.952796
638	6.2180447	10.95268
640	6.4547571	13.549134
800	5.7158749	9.3088684
800	5.7158749	9.3088684
805	5.1524623	8.3020868
805	5.1524623	8.3020529
810 B	5.1662935	8.320744
810 B	5.166334	8.3208273
810 M	5.3366771	8.9805324
810 M	5.3366771	8.9805324
815 B	5.2628912	10.434542
815 B	5.2628619	10.451851
815 M	5.3651255	12.006181
815 M	5.3651255	12.006315
815 E	5.8468804	13.118519
815 E	5.8468804	13.118519
820	6.0901454	13.432265
820	6.0900336	13.490592
822	6.2892547	13.537187
822	6.2892203	13.537289
825	6.8968736	10.650437

214	8.6497894	18.891922
322	7.0546833	11.900655
322	7.0546833	11.900655
326 B	7.3554734	9.6145431
326 B	7.2352558	9.6145431
326 M	7.3058349	9.1636999
326 M	7.605257	9.232953
326 E	7.7419177	9.8984831
326 E	7.7052035	9.9156199
328 B	7.8333652	9.9205456
328 B	7.912834	9.9949405
328 M	8.2738851	10.915342
328 M	7.9881243	10.915342
328 E	8.1464338	11.156846
328 E	8.0220912	11.156393
332	8.0339007	11.219414
332	7.2641944	11.505724
334	6.1235217	13.039712

Table 4-9. Load Points for RHR Lines

Unit 3		
NODE POINTS	NOP (ksi)	MAX (ksi)
5	9.771646	16.02175
10	8.81243	13.662224
10	8.812194	13.66267
15B	8.33433	12.433241
15B	8.334239	12.433202
15M	8.193514	12.21
15M	8.193514	12.21
15E	7.862934	11.812618
15E	7.445539	12.308857
20B	7.412785	11.517703
20B	7.412785	11.517657
20M	7.419432	11.548954
20M	7.419432	11.548954
20E	6.980055	11.030674
20E	6.980055	11.030674
25	4.87816	9.8406019
25	4.87816	9.8406019
30	7.179935	9.4883349
30	7.179935	9.4883349
35	7.653121	9.8729014
35	7.653121	9.8255048
40	8.01412	10.127955

Unit 4		
NODE POINTS	NOP (ksi)	MAX (ksi)
90	9.359497	11.26326
90	9.359497	11.26326
90	9.359497	11.26326
100	9.745627	12.21927
110	10.32247	13.83366
110	10.32247	13.83366
110	10.32247	13.83366
C7A	11.03248	15.74399
C7A	11.03248	15.74399
C7A	11.03248	15.74399
C7B	11.33993	16.88578
C7B	11.33993	16.88578
C7B	11.33993	17.00477
C8A	11.13434	16.7923
C8A	11.13434	16.7923
C8A	11.13434	16.53698
C8B	10.94254	16.6974
C8B	10.94254	16.6974
C8B	10.94254	16.6974
120	10.8842	17.37851

Table 4-10. Loads for Units 3 and 4 Pressurizer Surge Lines

NODE POINTS(1)	NOP (ksi)	MAX (ksi)
Pipe	23.910	24.732
Nozzle(2)	12.323	16.822

Notes:
(1) Node points correspond to one bounding location each on the 12" pipe and the 14" pipe at the nozzle end.
(2) To calculate bending stresses, thickness of thermal sleeve is neglected.

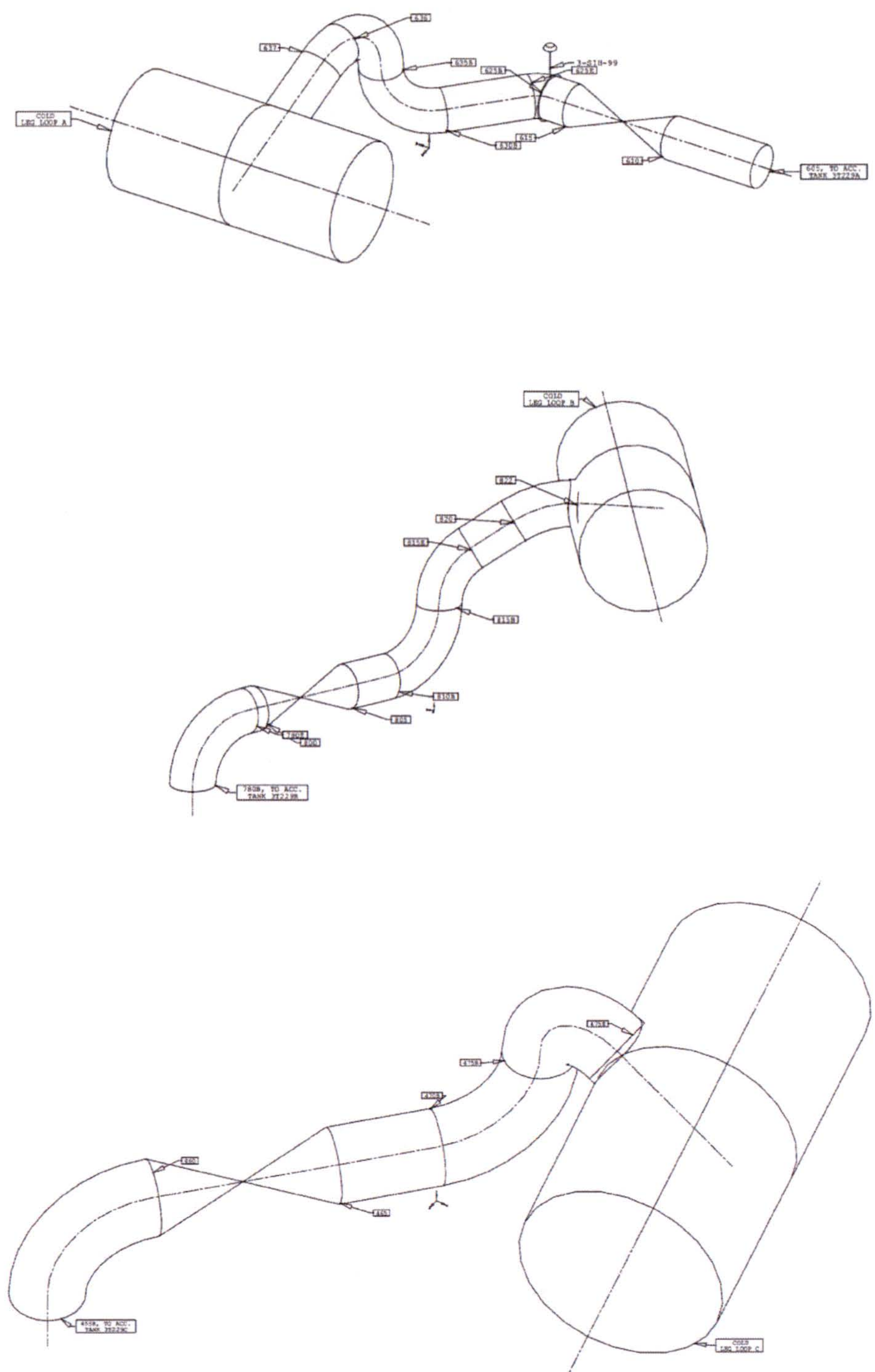

Figure 4-1. Schematic of Piping Model and Selected Node Points for Accumulator Lines (Loops A, B and C), PTN Unit 3 [34, 35, 36]

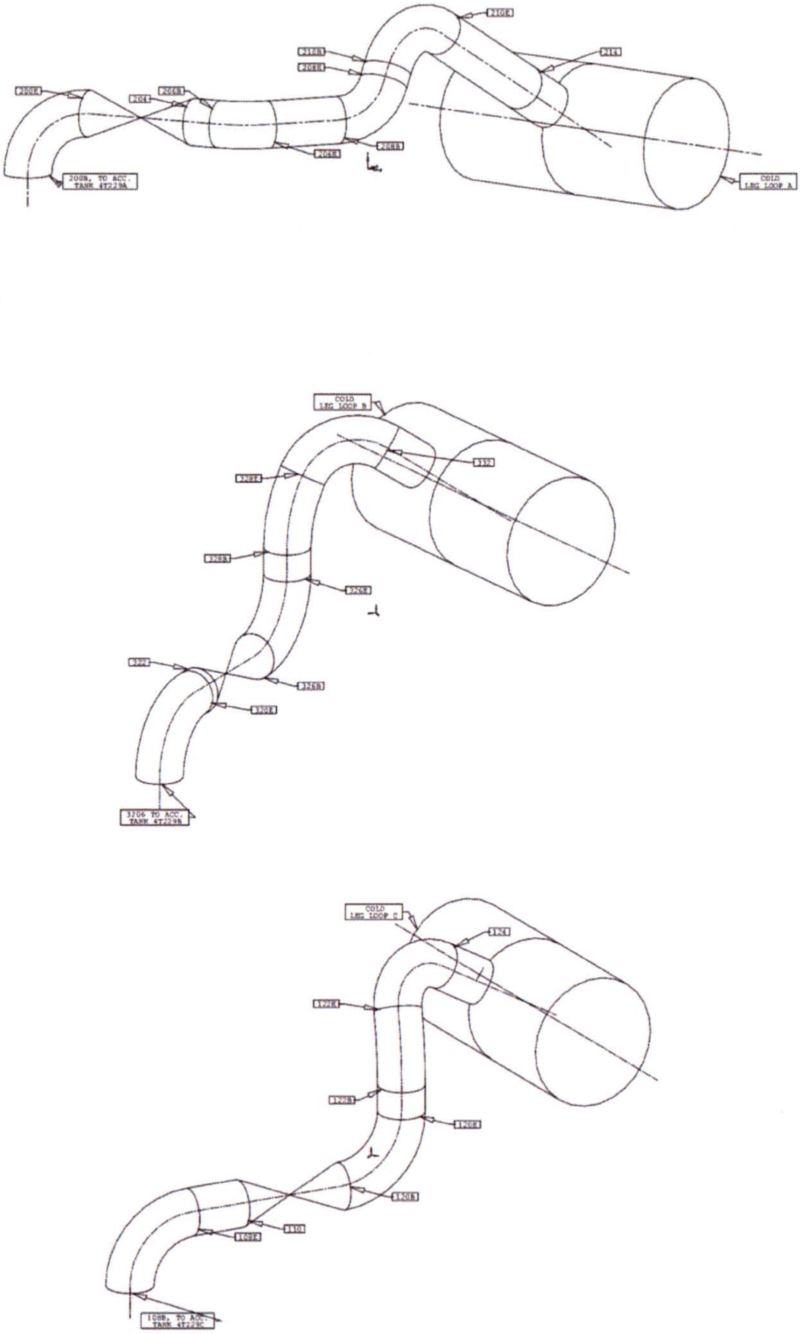

Figure 4-2. Schematic of Piping Model and Selected Node Points for Accumulator Lines (Loops A, B and C), PTN Unit 4 [39, 40, 41]

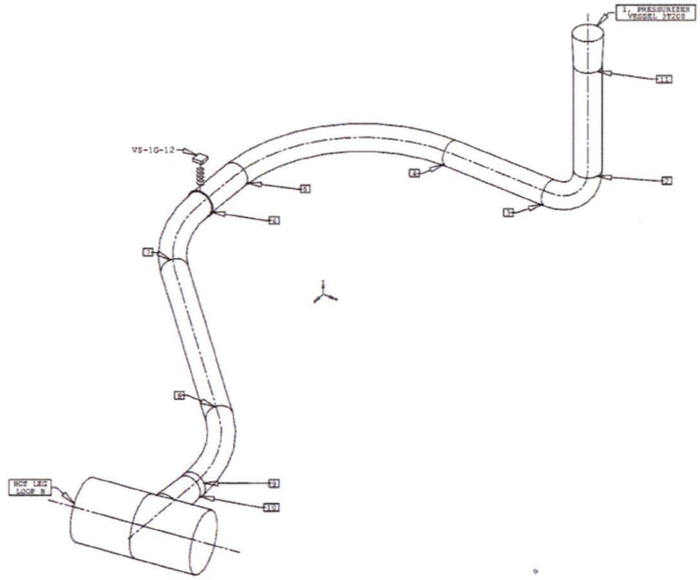

Figure 4-3. Schematic of Piping Model and Selected Node Points for Pressurizer Surge Line, PTN Unit 3 [38]

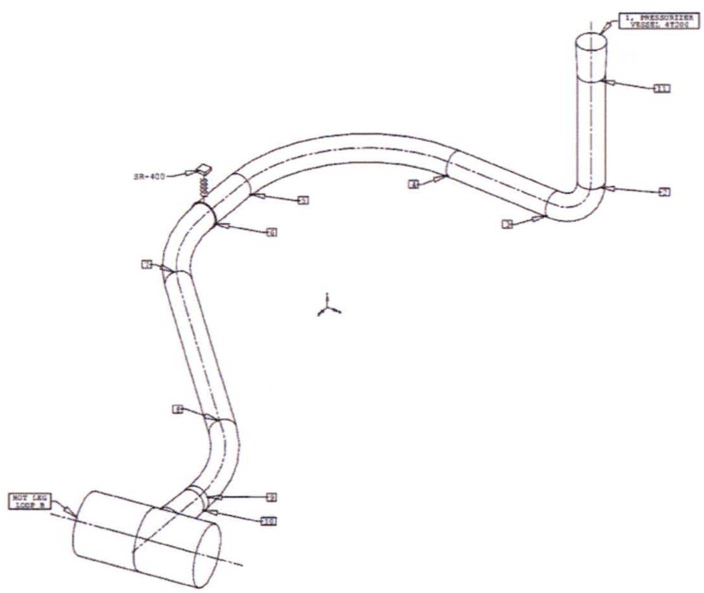

Figure 4-4. Schematic of Piping Model and Selected Node Points for Pressurizer Surge Line, PTN Unit 4 [43]

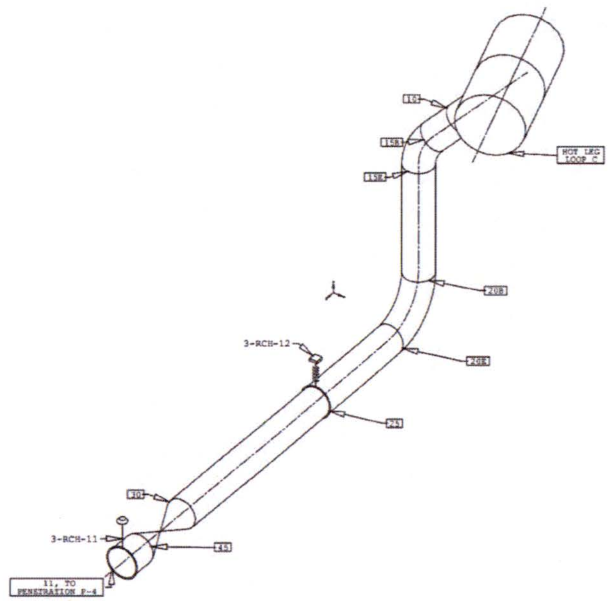

Figure 4-5. Schematic of Piping Model and Selected Node Points for RHR Line, PTN Unit 3 [37]

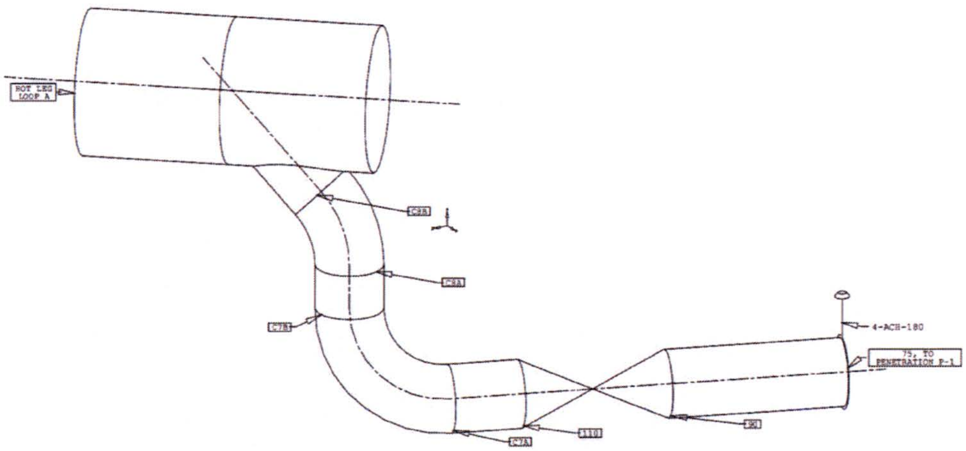

Figure 4-6. Schematic of Piping Model and Selected Node Points for RHR Line, PTN Unit 4 [42]

5.0 LEAK-BEFORE-BREAK EVALUATION

The LBB approach involves the determination of critical flaw sizes and leakage through flaws. The critical flaw length for a through-wall flaw is that length for which, under a given set of applied stresses, the flaw would become marginally unstable. Similarly, the critical stress is that stress at which a given flaw size becomes marginally unstable. NUREG-1061, Vol. 3 [6] defines required margins of safety on both flaw length and applied stress. Both of these criteria have been examined in this evaluation. Circumferential flaws are more restrictive than axial flaws since axial flaws are only affected by pressure stress and thus have larger critical flaw sizes with larger crack opening areas for leakage due to out of plane displacements. In this evaluation, only circumferential flaws are considered for all the piping systems.

5.1 Evaluation of Critical Flaw Sizes

Critical flaw sizes may be determined using either limit load/net section collapse criterion (NSCC) approach or J-Integral/Tearing Modulus (J/T) methodology. In this evaluation, as permitted by NUREG-0800, SRP 3.6.3, the limit load methodology was used to determine the critical flaw sizes since the piping material for all the piping systems under consideration is stainless steel which is ductile.

The methodology provided in NUREG-0800 [7] for calculation of critical flaw sizes by net section collapse (NSC-limit load) analysis was used to determine the critical flaw sizes. This methodology involves constructing a master curve where a stress index, SI, given by

$$SI = S + M P_m \tag{5-1}$$

is plotted as a function of postulated total circumferential through-wall flaw length, L, defined by

$$L = 2\,\theta\,R \tag{5-2}$$

where

$$S = \frac{2\,\sigma_f}{\pi}[2\sin\beta - \sin\theta] \qquad (5\text{-}3)$$

$$\beta = 0.5\,[(\pi - \theta) - \pi\,(P_m / \sigma_f)], \qquad (5\text{-}4)$$

θ	=	half angle in radians of the postulated through-wall circumferential flaw,
R	=	pipe mean radius, that is, the average between the inner and outer radius,
P_m	=	the combined membrane stress, including pressure, deadweight, and seismic components,
M	=	the margin associated with the load combination method (that is, absolute or algebraic sum) selected for the analysis. Since the absolute sum of the moments was used here, a value of 1.0 recommended in Reference 7 was used.
σ_f	=	flow stress for stainless steel pipe material categories.

If $\theta + \beta$ from Eqs. (5-1) and (5-5) is greater than π, then

$$S = \frac{2\sigma_f}{\pi}[\sin\beta], \qquad (5\text{-}5)$$

where

$$\beta = -\,\pi\,(P_m/\sigma_f) \qquad (5\text{-}6)$$

The critical flaw sizes correspond to the value of θ that result is S being greater than zero from Eqs. 5-3 and 5-5.

The value of SI used to enter the master curve for piping material is

$$SI = M\,(P_m + P_b) \qquad (5\text{-}7)$$

where

P_b = the combined primary bending stress, including deadweight and seismic components

The value of SI used to enter the master curve for SMAW and SAW is

$$SI = M (P_m + P_b + P_e) Z \qquad (5\text{-}8)$$

where

P_e = combined thermal expansion stress at normal operation,

Z = $1.15 [1.0 + 0.013 (OD\text{-}4)]$ for SMAW, (5-9)

Z = $1.30 [1.0 + 0.010 (OD\text{-}4)]$ for SAW, (5-10)

OD = pipe outer diameter in inches.

Since SMAW weld has a lower toughness (i.e., higher Z factor) than GTAW/TIG welds, it is assumed to be the only weld process used for all the cases. The leakage size was determined as one half the flaw size based on the master curve.

The maximum stress versus critical flaw size (2a) are plotted in Figure 5-1 through Figure 5-6. Figure 5-7 shows the maximum stress versus critical flaw size (2a) using a Z factor of 1.0 for base materials (pipe/elbow) of accumulator lines.

5.2 Leak Rate Determination

The determination of leak rate is performed using the EPRI program, PICEP [28]. The flow rate equations in PICEP are based on a modification of Henry's homogeneous non-equilibrium critical flow model [29]. The program accounts for non-equilibrium mass transfer between liquid and vapor phases, fluid friction due to surface roughness and convergent flow paths. The model was validated for steam and water leakage conditions [28].

In the determination of leak rates using PICEP, the following assumptions are made:

- A plastic zone correction is included in calculating the crack opening displacement. This is consistent with fracture mechanics principles for ductile materials.
- The crack is assumed to be elliptical in shape. This is the most appropriate representation for a crack that has the maximum crack opening displacement at the center of the crack that is available in PICEP for calculations of leakage.
- Crack roughness is taken as 0.000197 inches [30].
- There are no turning losses included since there are no mechanisms to cause intergranular cracking in the piping.
- The cracks are assumed to have a constant through wall depth and include a sharp-edged entrance loss factor of 0.61 (PICEP default).
- The default friction factors of PICEP are utilized.
- The crack opening area at the inlet and outlet are the same.
- The stress combinations included those for NOP conditions.

The leakage flaw sizes with respect to the leak rate of 2, 5 and 10 GPM were calculated for the operating pressures and temperatures shown in Tables 4-1 and 4-2 as appropriate using different moment stresses ranging from 0 to 45 ksi and material properties from Tables 4-5 and 4-7. The leakage flaw size curves are plotted in Figure 5-8 through Figure 5-13.

5.3 Bounding Analysis Curves

The bounding analysis curves (BACs) represent the maximum allowable membrane (pressure) plus bending stress (as determined from piping analysis for the system) as a function of the applied membrane (pressure) plus bending stress during normal plant operation. The latter condition represents the conditions during which leakage would have to be detected.

To determine a BAC point, the following steps are taken:

- A normal operating stress (membrane plus bending) is assumed.

- Using the curve of leakage flaw size versus normal condition applied stress, the crack length that will yield the required leakage rate (including the factor of 10 on top of the detectable leakage rate) is determined. This crack length is the total crack length (2a).
- The maximum allowable bending stress is determined from the curve of critical crack size (a) versus applied bending moment such that $a_{critical} = 2a_{leakage}$.
- This yields a point on the BAC curve for the maximum allowable.
- The BAC point so determined is corrected further, since it is based on shell theory stresses and the pipe bending stresses are determined in accordance with piping rules. The bending stress portion of the normal operating stress and the maximum stress must be corrected by the factor:

$$P_{b,BAC} = P_{b,analysis} \times (\pi R^2 t) / (2I/D)$$

where $P_{b,analysis}$ = bending stress prior to correction

R = mean radius of pipe

t = pipe wall thickness

I = pipe section moment of inertia

D = pipe outside diameter

This process is completed for the complete range of bending stresses from zero to ~50 ksi. The BAC curve so developed contains no other limitation. Membrane stress due to pressure (P) is calculated using the following formula:

$$\sigma_m = \frac{P\pi(R_{in})^2}{2\pi R_m t}$$

R_m = mean pipe radius
t = pipe wall thickness
R_{in} = inside radius of pipe.

The calculated BACs for Accumulator Line, RHR Line and Surge Lines are plotted in Figure 5-14 through Figure 5-19, respectively. Load points were calculated based on the loads listed in Table 4-8 through Table 4-17 for both Units 3 and 4. The corresponding load points for each of the pipe lines are plotted in Figure 5-14 through Figure 5-19 as well.

5.4 LBB Evaluation Results and Discussions

From the BACs and load points plotted in Figure 5-14 to Figure 5-19 all the stress points for both Units 3 and 4 are below 10 GPM BACs except for stress point 210M in the Unit 4 Accumulator Line as shown in Figure 5-14. Since the stress point 210M is in the middle of an elbow, the conservatism in using the weld material Z factor for pipe/elbow base material can be removed by using a Z factor of 1.0 (base material) instead of 1.444 (weld material). The maximum stress versus critical flaw size curve and the BAC plotted using a Z factor of 1.0 are shown in Figure 5-7 and Figure 5-20, respectively. With this change, it can be shown that stress point 210M is under the 10 GPM BAC and meets the LBB requirement.

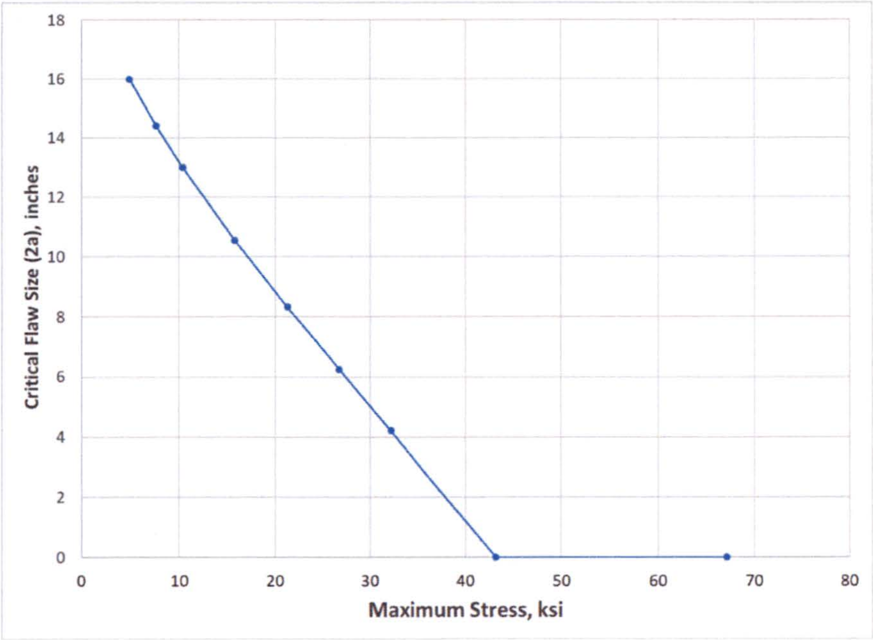

Figure 5-1. Maximum Stress versus Critical Flaw Size for Accumulator Lines (Z Factor=1.444)

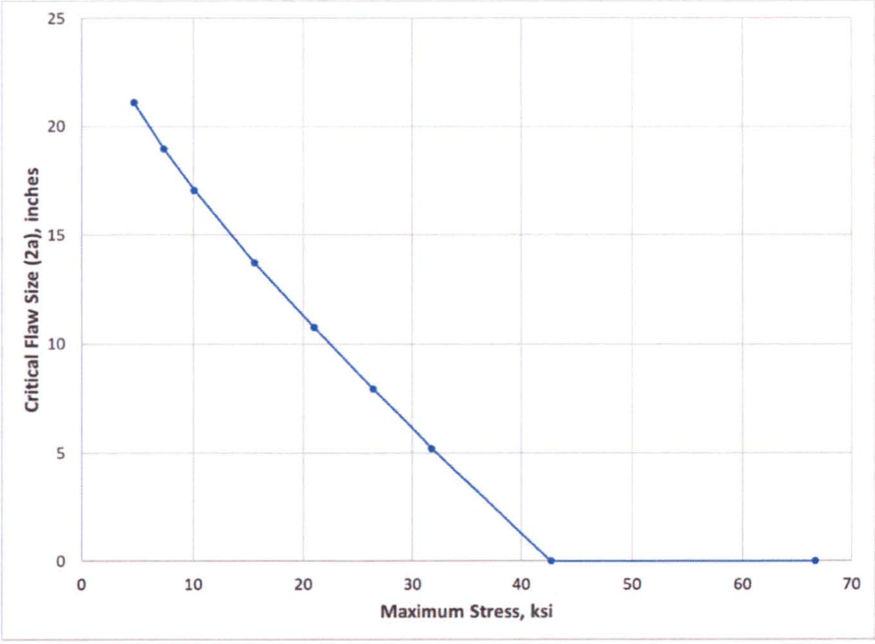

Figure 5-2. Maximum Stress versus Critical Flaw Size for RHR Lines (Z Factor=1.482)

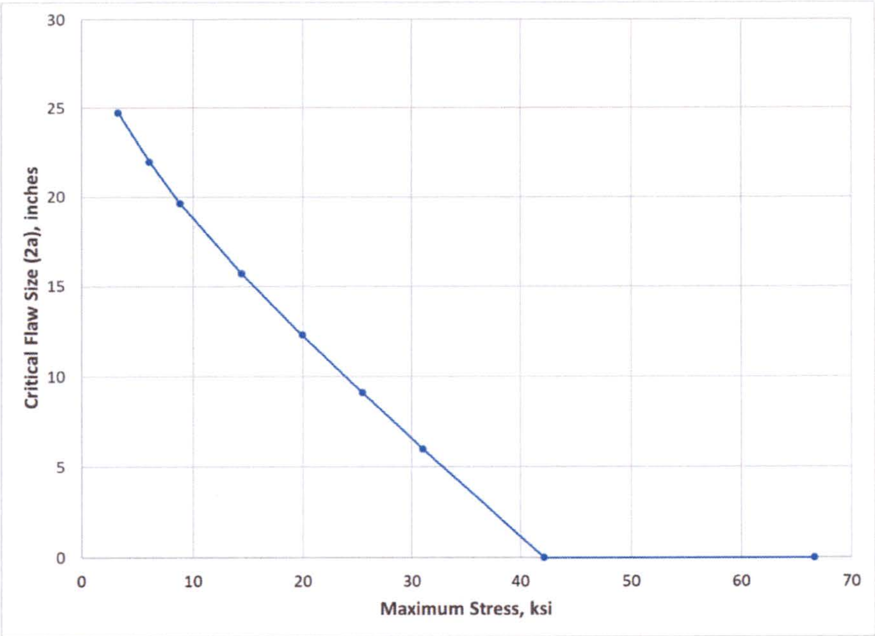

Figure 5-3. Maximum Stress versus Critical Flaw Size for Pressurizer Surge Line (Nozzle Side at Pressurizer End, Z Factor=1.5)

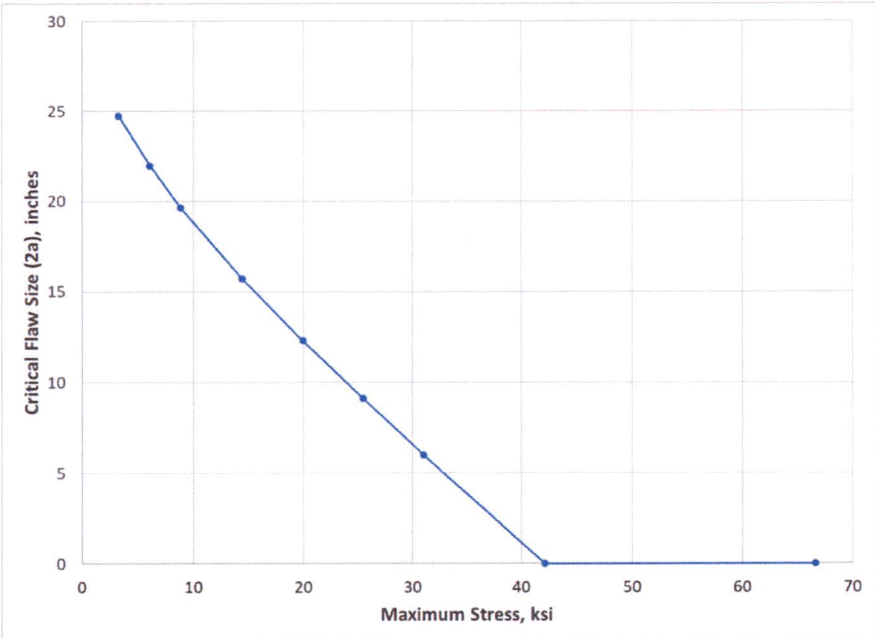

Figure 5-4. Maximum Stress versus Critical Flaw Size for Pressurizer Surge Line (Nozzle Side at Hot Leg End, Z Factor=1.5)

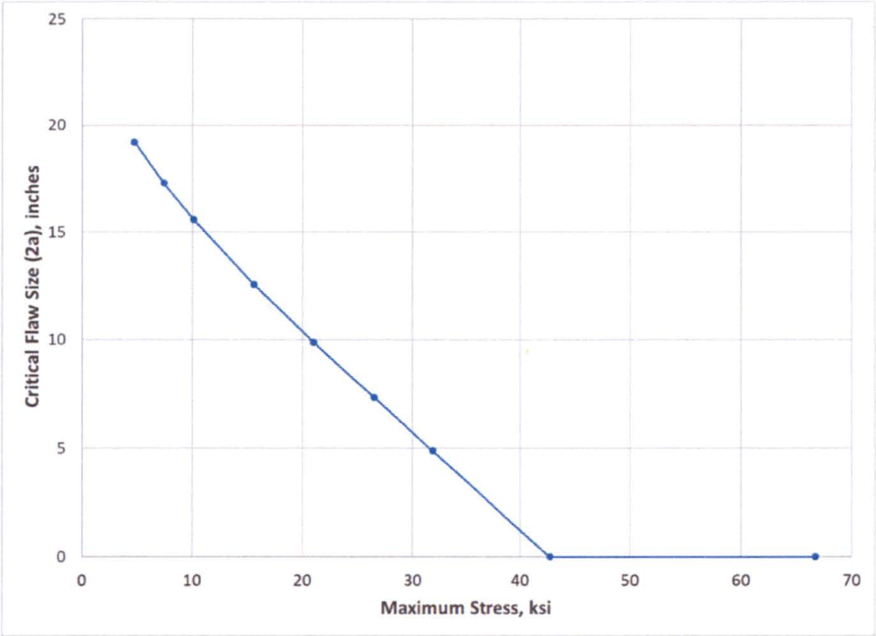

Figure 5-5. Maximum Stress versus Critical Flaw Size for Pressurizer Surge Line (Pipe Side at Pressurizer End, Z Factor=1.466)

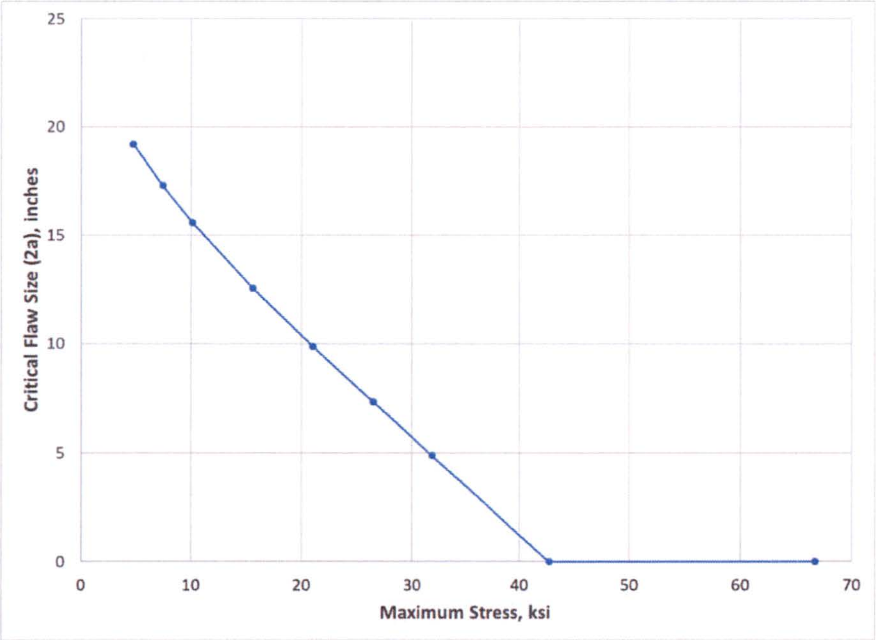

Figure 5-6. Maximum Stress versus Critical Flaw Size for Pressurizer Surge Line (Pipe Side at Hot Leg End, Z Factor=1.466)

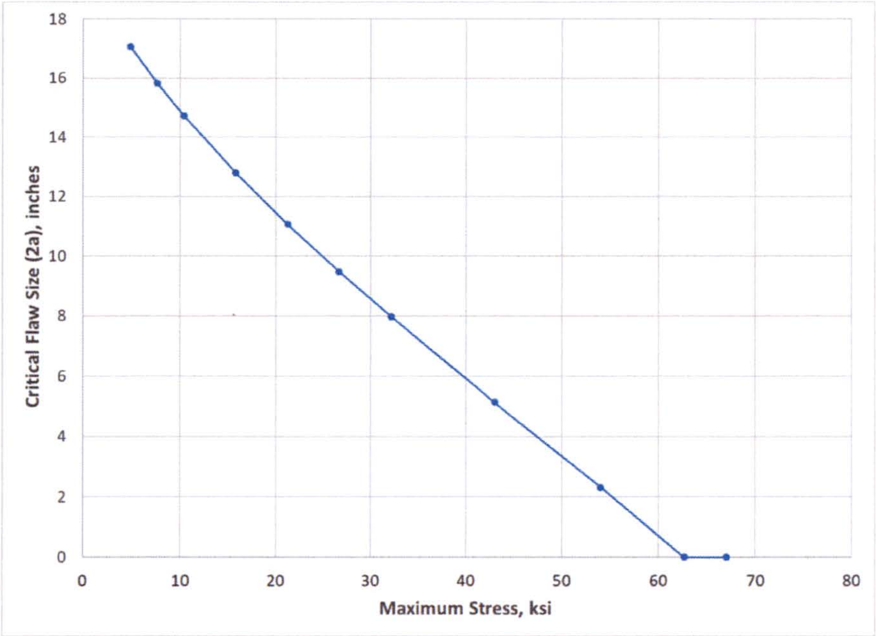

Figure 5-7. Maximum Stress versus Critical Flaw Size for Pipe/Elbow of Accumulator Lines (Z Factor=1.0)

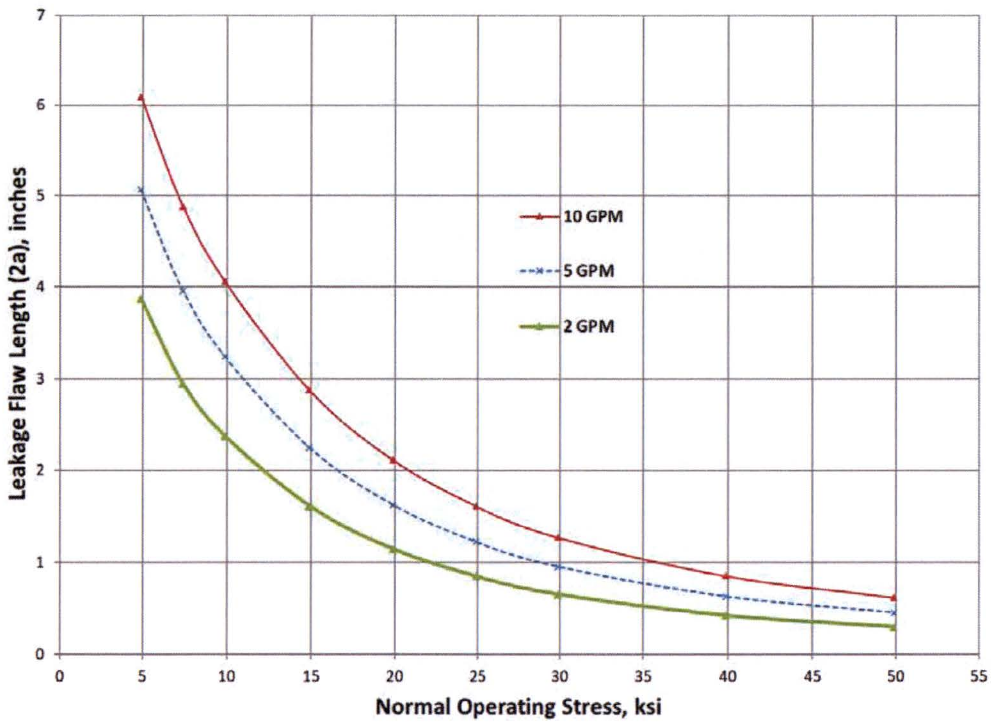

Figure 5-8. Leakage Flaw Size versus Normal Operating Stress of Accumulator Lines

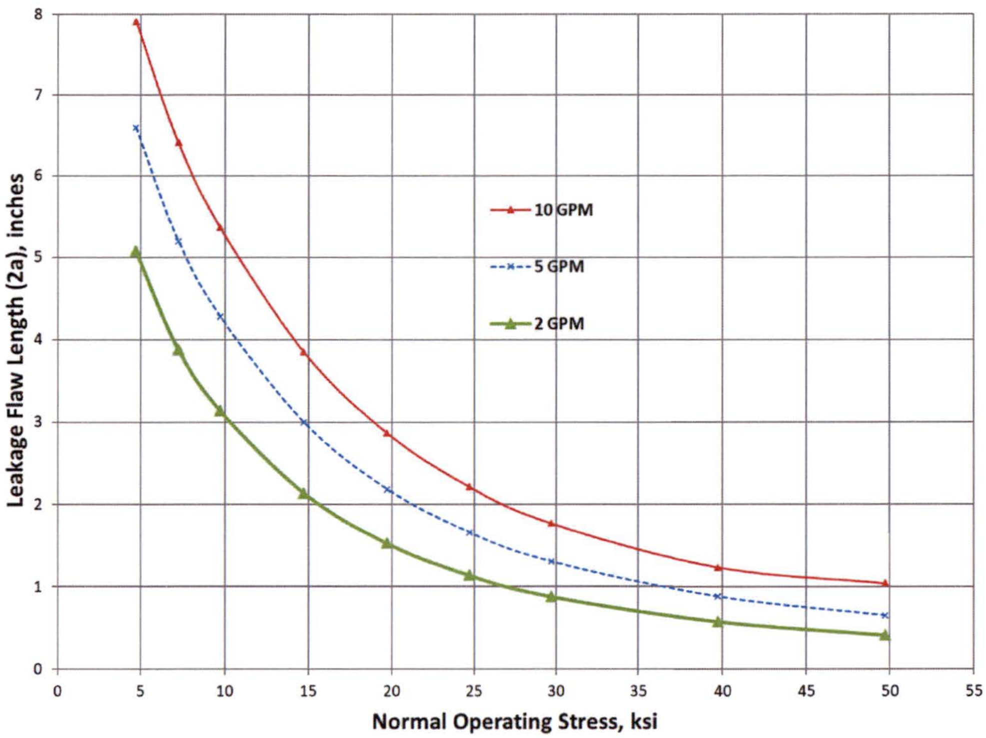

Figure 5-9. Leakage Flaw Size versus Normal Operating Stress of Pressurizer Surge Lines (Pipe Side at Pressurizer End)

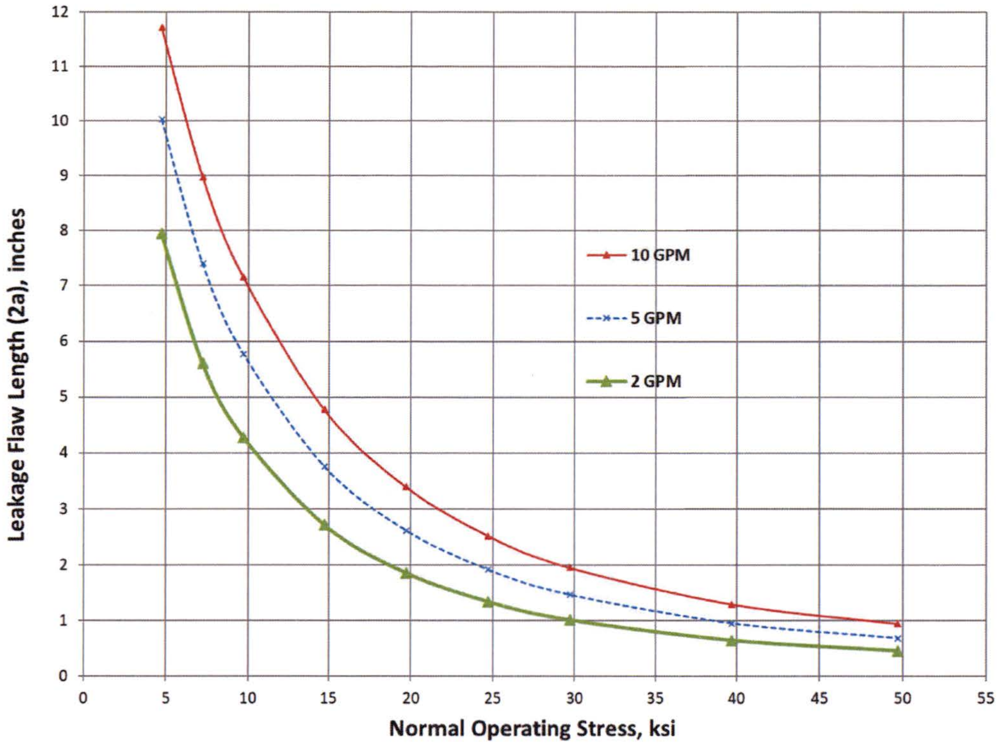

Figure 5-10. Leakage Flaw Size versus Normal Operating Stress of Pressurizer Surge Lines (Nozzle Side at Pressurizer End)

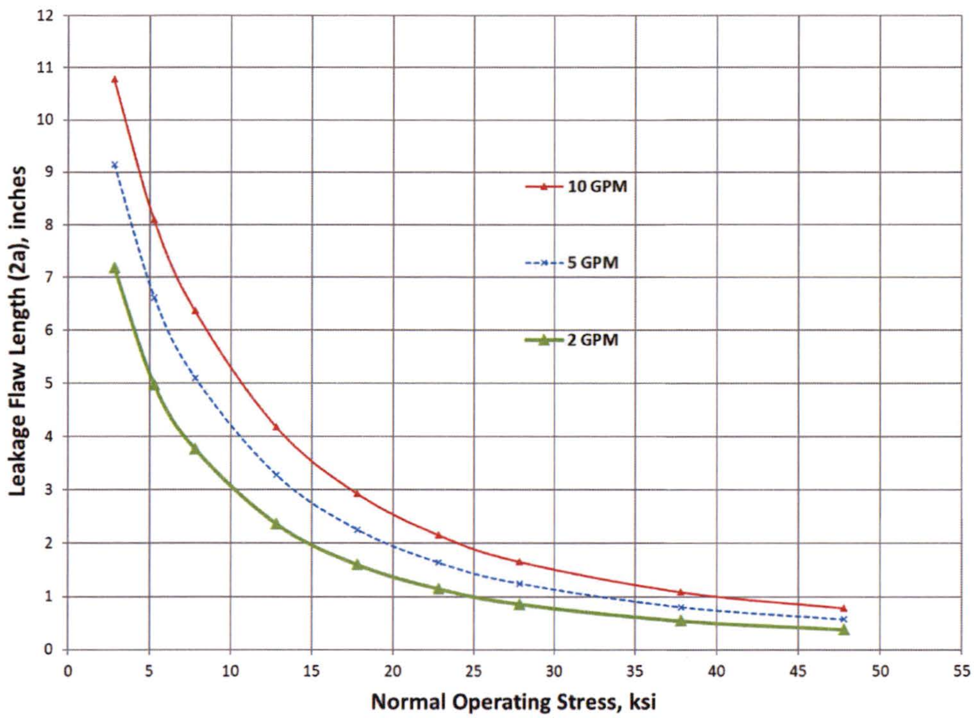

Figure 5-11. Leakage Flaw Size versus Normal Operating Stress of Pressurizer Surge Line (Nozzle Side at Hot Leg End)

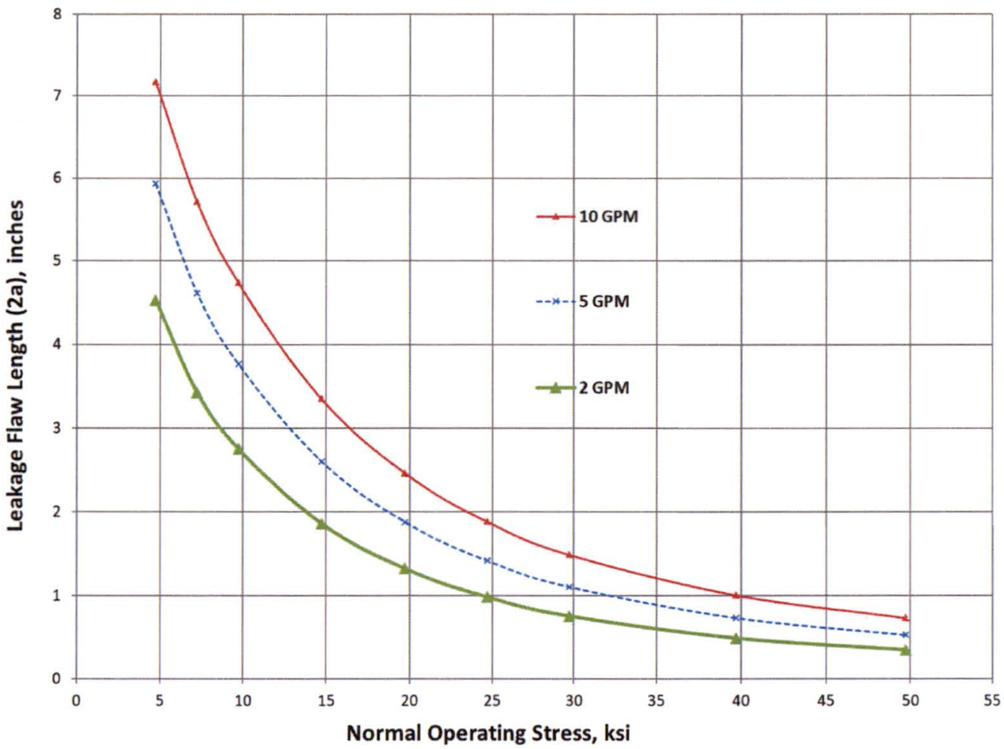

Figure 5-12. Leakage Flaw Size versus Normal Operating Stress of Pressurizer Surge Line at Hot Leg End

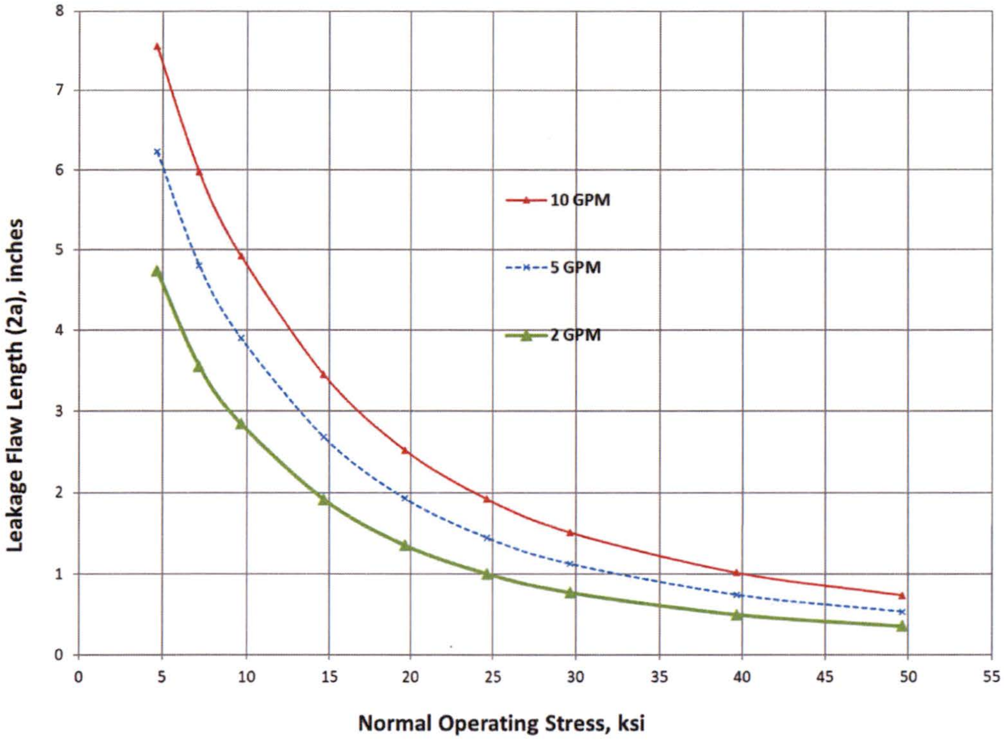

Figure 5-13. Leakage Flaw Size versus Normal Operating Stress of RHR Line at Hot Leg End

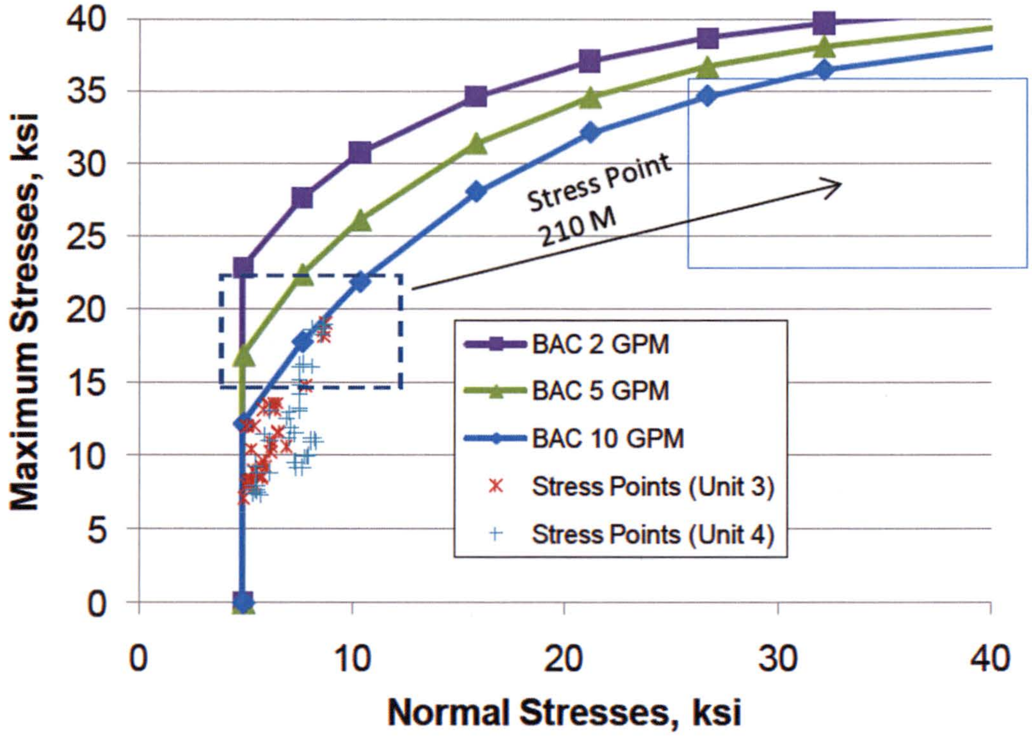

Figure 5-14. BACs and Load Points for Accumulator Lines

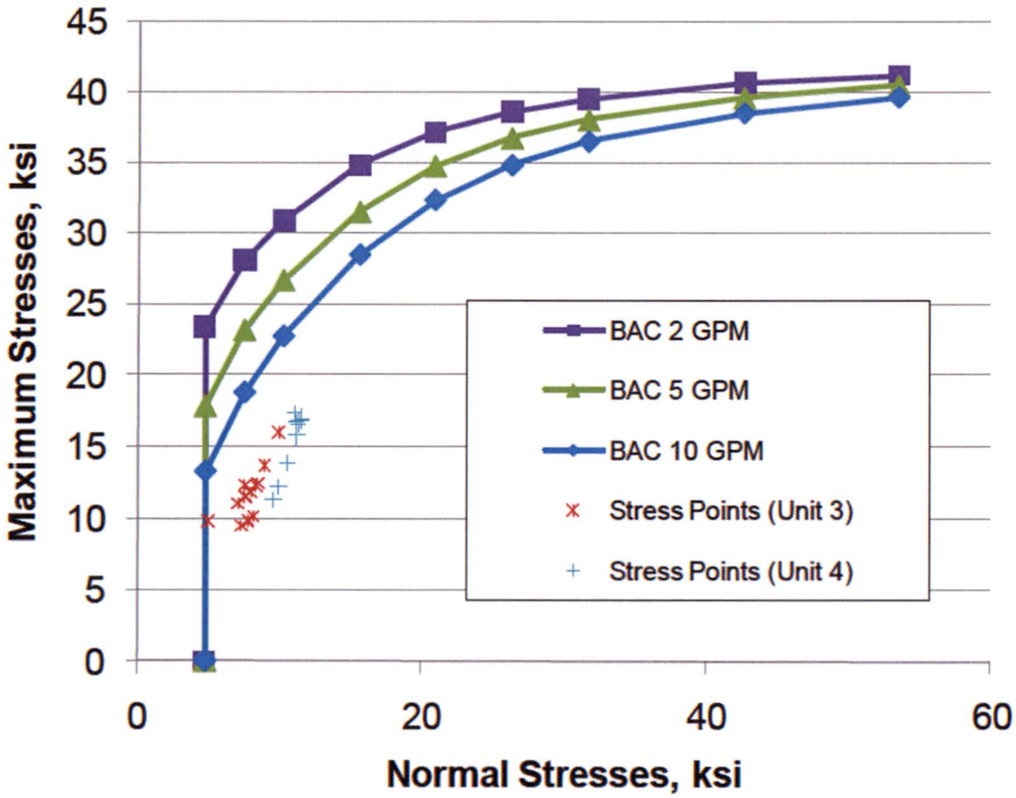

Figure 5-15. BACs and Load Points for RHR Lines

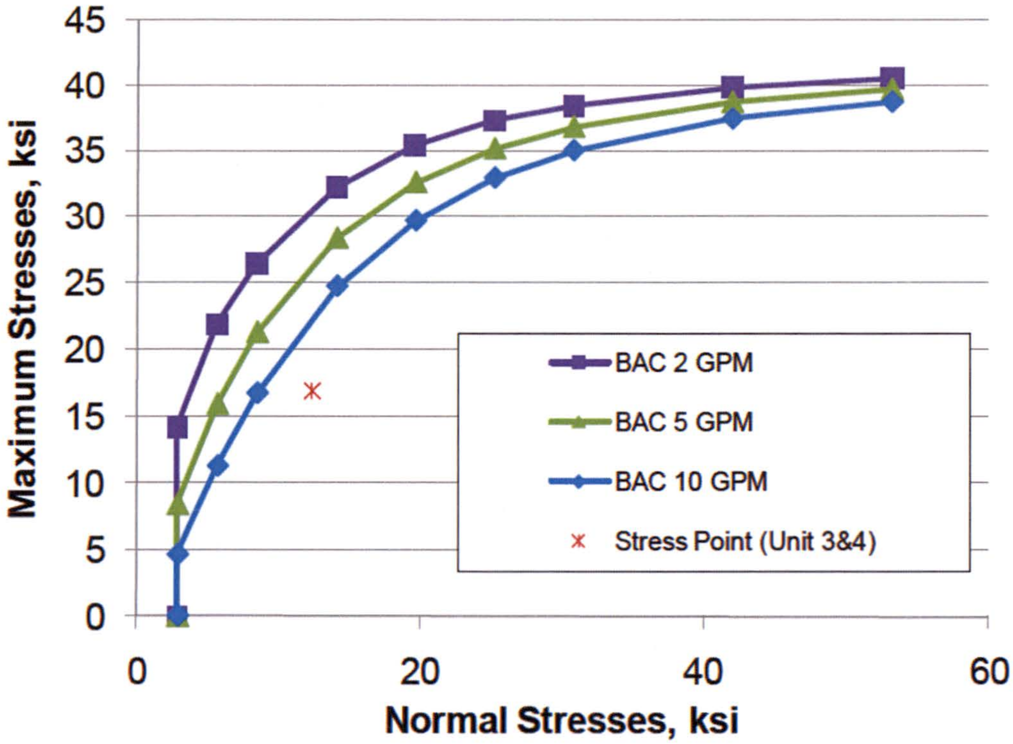

Figure 5-16. BACs and Load Point for Pressurizer Surge Lines (Nozzle Side at Pressurizer End)

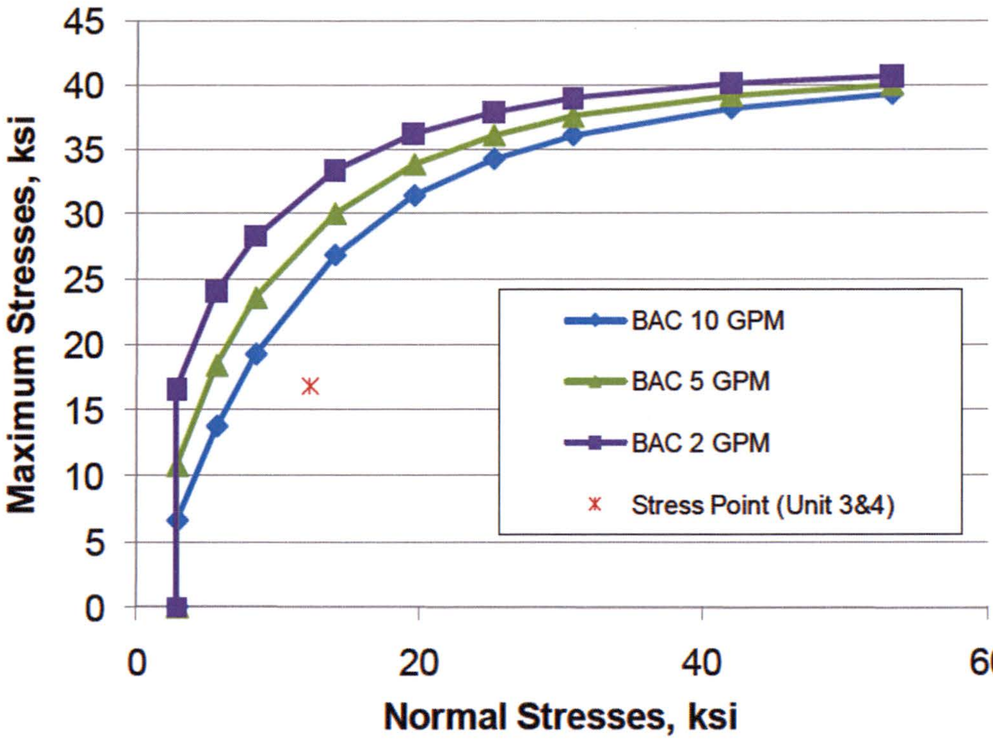

Figure 5-17. BACs and Load Point for Pressurizer Surge Line (Nozzle Side at Hot Leg End)

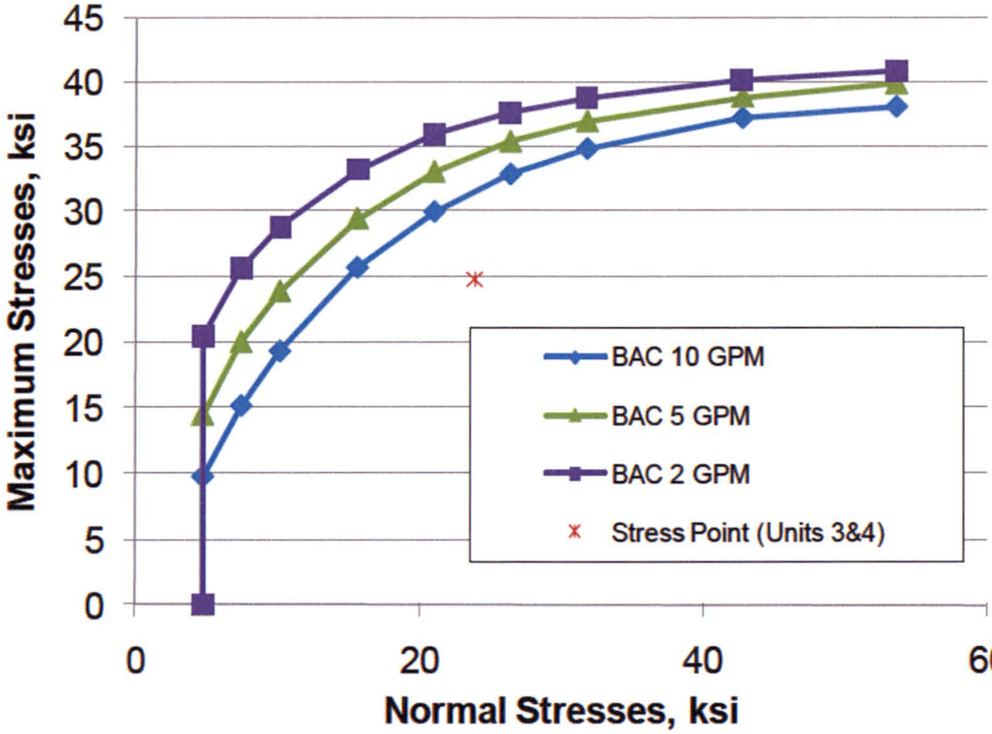

Figure 5-18. BACs and Load Point for Pressurizer Surge Lines (Pipe Side at Pressurizer End)

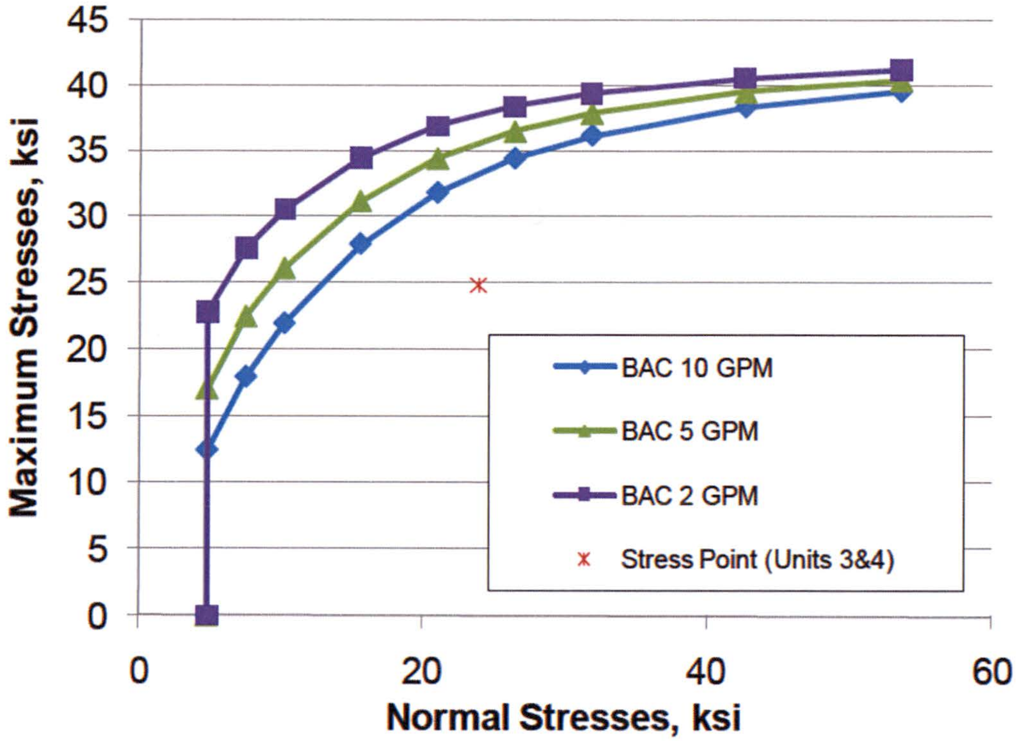

Figure 5-19. BACs and Load Point for Pressurizer Surge Lines (Pipe Side at Hot Leg End)

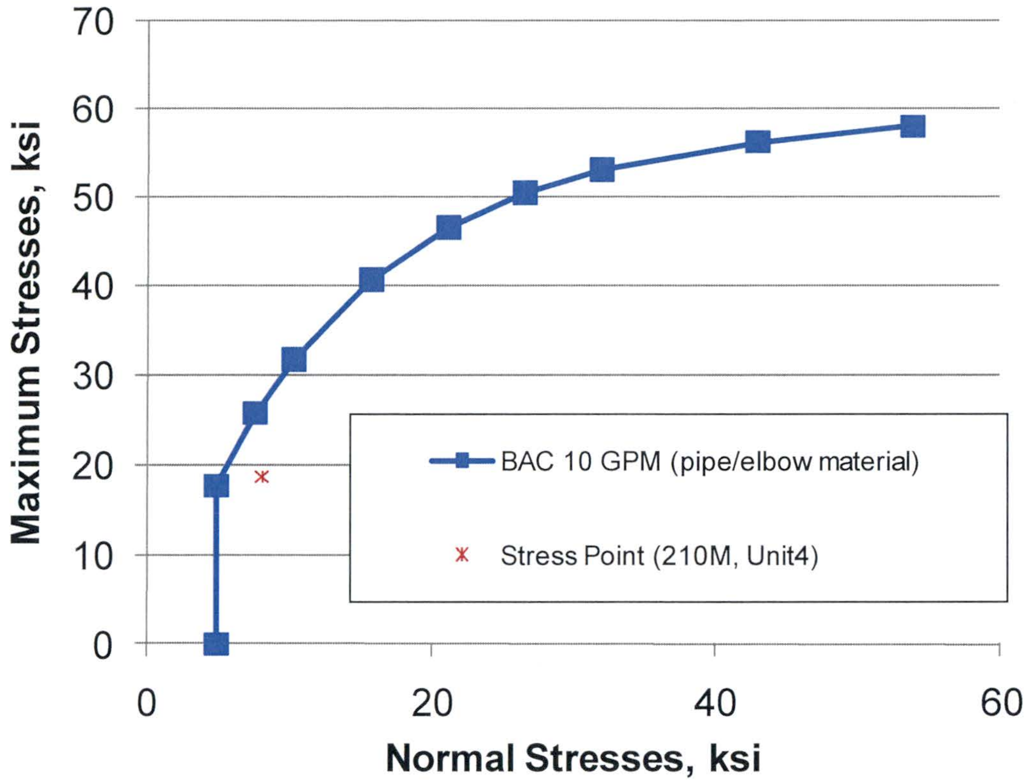

Figure 5-20. 10 GPM BAC Curve for Pipe/Elbow (Z Factor=1.0) of Accumulator Lines

6.0 EVALUATION OF FATIGUE CRACK GROWTH OF SURFACE FLAWS

In accordance with the NRC criteria [6] set forth in Section 2 of this report, the growth of postulated surface cracks by fatigue is evaluated to demonstrate that such growth is insignificant for the plant life, when initial flaw sizes meeting ASME Code Section XI IWB-3514 acceptance standards [26] are postulated.

6.1 Plant Transients

Since PTN RCS attached piping lines were designed to the requirements of ANSI B31.1, no specific line unique transients exist in the design basis. Hence, transient information from generic U. S. Pressurized Water Reactor (PWR) Operational Transients [31] was obtained to perform the crack growth evaluation. The plant transients for crack growth affecting the auxiliary lines of PTN Units 3 and 4, provided in Reference [31], are presented in Table 6-1 for the Accumulator Line and in Table 6-2 for the Residual Heat Removal (RHR) Line.

In addition, the Surge Line experiences thermal stratification which results in larger stress ranges, thus more fatigue growth during transients. A Westinghouse fatigue calculation [50] was conducted considering thermal stratification during the transients. The definition of transients for crack growth, number of cycles, as well as the stress range for each transient are obtained from this calculation, and reproduced in Table 6-3.

6.2 Stresses for Crack Growth Evaluation

The axial stresses due to pressure and thermal loads are calculated as described below. For pressure loads, P, the axial stress is calculated as:

$$\sigma_p = P \frac{D_i^2}{D_o^2 - D_i^2}$$

where D_o is the outside diameter and D_i is the inside diameter of the pipe.

Bending stress is given by $\sigma_b = D_o(M)/2I$,

where

M = bending moment

I = moment of inertia

$= (\pi/64)\times(D_o^4 - D_i^4)$

For thermal expansion moments, the maximum operating thermal moments ($M_{max\ oper}$), from Section 4, are scaled by the ratio of the transient temperature range (ΔT) to the operating temperature range (ΔT_{oper}):

$$M_t = M_{max\ oper}\ (\Delta T/\Delta T_{oper}),$$

where ΔT_{oper} is based on the temperatures at which the thermal expansion moments were calculated. $\Delta T_{oper} = T_{oper} - 70$. The operating temperature for the Accumulator and RHR Lines are obtained from Section 4.0. The temperature range for the transients of the Accumulator and RHR Lines are obtained from Reference [31] and reproduced in Table 6-1 and Table 6-2, respectively.

For the Accumulator and RHR Lines, the moments from deadweight, thermal and operating basis earthquake (OBE) are obtained as the maximum moments from Tables 4-7 through Table 4-15 and shown in Table 6-4. The calculated maximum and minimum axial pressure, thermal, and dead weight stresses for each of the plant transients are presented in Table 6-5 for the Accumulator Line and Table 6-6 for the RHR Line. The computed stress ranges for transients using Table 6-5 and Table 6-6 are presented in Table 6-7 and Table 6-8 for the Accumulator and RHR Lines, respectively. For the Surge Line, the stress ranges are computed from maximum and minimum stresses in Table 6-3 and presented in Table 6-9.

For all the lines, the weld residual stress is conservatively represented by a pure through-wall bending stress equal to the yield stress of the pipe material at the operating temperature. Since

Accumulator, RHR and Surge Lines are made of materials of similar type, the most conservative yield stress was chosen for all three types of lines. Thus, $S_y = 18.28$ ksi of Material Type 316 at 653°F is used in this analyses.

The number of OBE event occurrences are 50, obtained from Reference [50]. This number is applicable to 80 years of operation per Reference 51. Note that OBE loads are conservatively assumed to be the same as SSE loads where OBE loads are not directly available.

6.3 Allowable Flaw Size

Since the stainless steel piping material behaves in a ductile manner, the net section plastic collapse methodology in Appendix C of ASME Code Section XI [26] can be used to determine the allowable flaw size. The load combination used for determining the allowable flaw size is pressure, deadweight, thermal expansion and seismic. The flow stress, σ_f for all three types of lines is conservatively assumed as 45.14 ksi (Type 316 at 653°F).

For the Accumulator Line, the total stress for this load combination is 19.02 ksi. The stress ratio $(\sigma_m+\sigma_b)/\ \sigma_f = 0.42$. With an aspect ratio a/l of 0.1 and a thickness of 1.0 inch, starting with the maximum allowable flaw depth-to-thickness ratio of 0.75, the maximum possible flaw length is 7.5 inches. The ratio of this flaw length to the pipe circumference is 0.22. Using Table C-5310-3 Table C-5310-4 for emergency and faulted conditions, the allowable end-of-evaluation period flaw depth-to- thickness ratio is determined to be 0.75.

For the RHR Line, the total stress for this load combination is 17.38 ksi. The stress ratio $(\sigma_m+\sigma_b)/\ \sigma_f = 0.55$. With an aspect ratio a/l of 0.1 and a thickness of 1.25 inch, starting with the maximum allowable flaw depth-to-thickness ratio of 0.75, the maximum possible flaw length is 9.34 inches. The ratio of this flaw length to the pipe circumference is 0.22. Using Table C-5310-3 Table C-5310-4 for emergency and faulted conditions, the allowable end-of-evaluation period flaw depth-to- thickness ratio is determined to be 0.70.

For the Surge Line, the total stress for this load combination is 24.73 ksi. The stress ratio $(\sigma_m+\sigma_b)/\sigma_f = 0.39$. With an aspect ratio a/l of 0.1 and a thickness of 1.125 inch, starting with the maximum allowable flaw depth-to-thickness ratio of 0.75, the maximum possible flaw length is 8.44 inches. The ratio of this flaw length to the pipe circumference is 0.21. Using Table C-5310-3 Table C-5310-4 for emergency and faulted conditions, the allowable end-of-evaluation period flaw depth-to- thickness ratio is determined to be 0.75.

6.4 Fatigue Crack Growth Analysis

The fatigue crack growth analysis is performed for the number of cycles corresponding to the 40-year design plant life shown in Section 6.1. These cycles are applicable to both 60 years of operation per Reference [55], and 80 years of operation per Reference [51]. In the definition of the stress ranges, the stresses are cycled around the sum of deadweight and weld residual stresses, which are always in effect. For each enveloping transient category, the appropriate scaling factors (transient stress/reference stress) are input to obtain the actual K values for the fatigue crack growth.

6.4.1 Fatigue Crack Growth Law Used for 60-Year Operation Calculations

Crack growth in stainless steel for 60 years is calculated using the austenitic steel fatigue crack growth law in air from Article C-3210 of the ASME, Section XI [26]. Reference [33] indicates a factor of 2 may be applied to account for a PWR environment. This is accounted for in **pc-CRACK 4.1** [49a] by doubling the number of cycles.

$$(da/dN)_{air} = C_0(\Delta K)^n \text{, units of inch/cycle}$$

where:

da/dN	=	crack growth per cycle, a is the crack depth, N is the number of cycles
C_0	=	$C \cdot S$
C	=	$10^{\wedge}[-10.009 + 8.12\times10^{-4}T - 1.13\times10^{-6}T^2 + 1.02\times10^{-9}T^3]$
S	=	1.0 when $R \leq 0$
	=	1.0 + 1.8R when $0 < R \leq 0.79$
	=	-43.35 + 57.97R when $0.79 < R < 1.0$
T	=	metal temperature, °F (taken as the maximum during the transient)
R	=	R-ratio = (K_{min}/K_{max})

ΔK = $K_{max} - K_{min}$ = range of stress intensity factor, ksi-in$^{0.5}$
n = 3.3 per Section XI, Appendix C [26]

Note that for negative R-ratios ($K_{min} < 0$ and $K_{max} > 0$), the "S" value is 1.0, which could lead to over conservative crack growth for the stainless steel weld. The max C_0 and thus most conservative growth rate is used for each transient considered.

6.4.2 Fatigue Crack Growth Law Used for 80-Year Operation Calculations

Crack growth in stainless steel for 80 years uses the fatigue crack growth (FCG) law for stainless steels and associated weld metals from ASME Code Case N-809 [53]:

$da/dN = C_0 \cdot \Delta K^n$, units of inch/cycle

where:

C_0 = scaling parameter that accounts for the effect of loading rate and environment on fatigue crack growth rate
= $C\ S_T\ S_R\ S_{ENV}$
n = slope of the log (da/dN) versus log (ΔK) curve = 2.25
C = nominal fatigue crack growth rate constant
= 4.43×10^{-7} for $\Delta K \geq \Delta K_{th}$
= 0 for $\Delta K < \Delta K_{th}$
ΔK = stress intensity factor range, ksi$\sqrt{\text{in}}$
ΔK_{th} = 1.10 ksi$\sqrt{\text{in}}$
S_T = parameter defining effect of temperature on FCG rate
= e^{-2516/T_K} for $300°F \leq T \leq 650°F$
= $3.39 \times 10^5\ e^{[(-2516/T_K)-0.0301T_K]}$ for $70°F \leq T < 300°F$
T = metal temperature, °F
S_R = parameter defining the effect of R-ratio on FCG rate
= 1.0 for $R < 0$
= $1 + e^{8.02(R-0.748)}$ for $0 \leq R < 1.0$
R = K_{min}/K_{max} = R ratio
S_{ENV} = parameter defining the environmental effects on FCG rate
= $T_R^{0\,3}$
T_R = loading rise time, sec
T_K = $[(T-32)/1.8+273.15]$, K

The metal temperature of 653°F is applied to calculate the crack growth rate. A conservative loading rise time of 15,000 seconds is applied to calculate the crack growth rate.

The crack growth rate changes based on the R-ratio. The da/dN for selected ΔK is calculated for different R-ratios and entered into **pc-CRACK 4.1** [49a] to calculate crack growth using Code Case N-809 FCG equation.

6.4.3 Part Through-Wall Crack Growth

The crack growth analysis is performed using the fracture mechanics software program **pc-CRACK 4.1** [49a]. Based on the guidelines of ASME Code Section XI, IWB-3514, an initial flaw size equal to the allowable depth of up to 12.5% of wall thickness is postulated. For the crack growth analysis, an aspect ratio a/l of 0.1 is conservatively assumed for the initial flaw, where 'a' is the flaw depth and 'l' is the flaw length.

The results are shown in Table 6-10. Considering the larger growth of 80 years using the crack growth law from ASME Code Case N-809, the results show that the postulated partial through wall crack (a/t = 0.125, a/l = 0.1) does not grow during the design plant life for the Accumulator Line. For the RHR Line, the postulated crack (a/t = 0.125, a/l = 0.1) grows only 0.0014 inch during the design plant life to a final a/t ratio of 0.1262. This final a/t ratio is less than the allowable ratio of 0.70 documented in Section 6.3. For the Surge Line, the postulated crack (a/t = 0.125, a/l = 0.1) grows 0.0855 inch during the design plant life to a final a/t ratio of 0.2010. This final a/t ratio is less than the allowable ratio of 0.75 documented in Section 6.3.

Hence, the integrity of the auxiliary line piping is not jeopardized between in-service inspections.

6.4.4 Through-Wall Crack Growth

NUREG-1061, Section 5.2 (g) [6] requires that an evaluation be performed to show that the leakage flaw size is stable during an SSE event. A very simple approach is taken to determine the crack growth of a through-wall leakage size flaw to demonstrate stability. The initial through-wall flaw is assumed to correspond to the leakage flaw length for the most limiting location. A crack model in **pc-CRACK 4.2** [49b] for a through-wall circumferential crack in a cylinder under tension and bending is used for the stress intensity K calculation. In this evaluation, the maximum $\sigma_m+\sigma_b$ is conservatively applied as tension stress in the **pc-CRACK 4.2** input.

For the Accumulator Line, the maximum $\sigma_m+\sigma_b$ is 19.02 ksi (including internal pressure), and the bounding half leakage flaw size (a_L) is 2.53 inches with bending stress= 0 for 5GPM (Figure 5-8). Note that the maximum stress for SSE event is sum of the operating stress and stress due to SSE loading. The minimum stress for SSE event is calculated by subtracting the stress due to SSE from the operating stress, which is -9.14 ksi. The resultant stress intensity factors K_{max} and K_{min} are 69.09 $ksi\sqrt{in}$ and -33.20 $ksi\sqrt{in}$ for the half leakage flaw size of 2.53 inch. Using a negative R ratio (K_{min}/K_{max}) in the ASME Code Section XI crack growth curve for stainless steels in a water environment (Figure C-8410-1) gives a crack growth per cycle of 1.81×10-3 inches, whereas for 80 years the ASME Code Case N-809 crack growth curve gives 4.51×10-3 inches per cycle. For the assumed 51 cycles of SSE (conservative representation of 1 SSE and 50 OBE cycles), this growth is 0.092 inches for the ASME Section XI crack growth law and 0.230 inches for the Code Case N-809 crack growth law. Final half flaw sizes (a_f) are 2.622 inches for the ASME Section XI crack growth law and 2.760 inches for the Code Case N-809 crack growth law. These final half flaw sizes are less than the critical half flaw size (a_c) of 4.61 inches with the maximum stress of 19.02 ksi.

For the RHR Line, the maximum $\sigma_m+\sigma_b$ is 17.38 ksi (including internal pressure), and the bounding half leakage flaw size (a_L) is 3.12 inches with bending stress= 0 for 5GPM (Figure 5-13). The minimum stress for SSE event is calculated by subtracting the stress due to SSE from the operating stress, which is -7.62 ksi. The resultant stress intensity factors K_{max} and K_{min} are 68.86 $ksi\sqrt{in}$ and -30.19 $ksi\sqrt{in}$ for the half leakage flaw size of 3.12 inch. Using a negative R ratio (K_{min}/K_{max}) in the ASME Code Section XI crack growth curve for stainless steels in a water environment (Figure C-8410-1), the crack growth per cycle is 1.62×10^{-3} inches, whereas for 80 years the ASME Code Case N-809 crack growth curve gives 4.19×10^{-3} inches per cycle. For the assumed 51 cycles of SSE (conservative representation of 1 SSE and 50 OBE cycles), this growth is 0.083 inches for the ASME Section XI crack growth law and 0.214 inches for the Code Case N-809 crack growth law. Final half flaw sizes (a_f) are 3.203 inches for the ASME Section XI crack growth law and 3.334 inches for the Code Case N-809 crack growth law. These final half flaw sizes are less than the critical half flaw size (a_c) of 6.35 inches with the maximum stress of 17.38 ksi.

For the Surge Line, the maximum $\sigma_m+\sigma_b$ is 24.73 ksi (including internal pressure), and the bounding half leakage flaw size (a_L) is 3.30 inches with bending stress= 0 for 5GPM (Figures 5-9 to 5-12). The calculated minimum stress is -0.09 ksi. The resultant stress intensity factors K_{max} and K_{min} are 107.35 $ksi\sqrt{in}$ and -0.39 $ksi\sqrt{in}$ for the half leakage flaw size of 3.30 inch. Using a negative R ratio (K_{min}/K_{max}) in the ASME Code Section XI crack growth curve for stainless steels in a water environment (Figure C-8410-1), the crack growth per cycle is 2.14×10^{-3} inches, whereas for 80 years the ASME Code Case N-809 crack growth curve gives 5.06×10^{-3} inches per cycle. For the assumed 51 cycles of SSE (conservative representation of 1 SSE and 50 OBE cycles), this growth is 0.109 inches for the ASME Section XI crack growth law and 0.258 inches for the Code Case N-809 crack growth law. Final half flaw sizes (a_f) are 3.409 inches for the ASME Section XI crack growth law and 3.558 inches for the Code Case N-809 crack growth law. These final half flaw sizes are less than the critical half flaw size (a_c) of 4.06 inches with the maximum stress of 24.73 ksi.

The through-wall crack growth results are summarized in Table 6-11. The results provided in this table demonstrate that in all cases the final flaw size does not reach the critical flaw size despite the conservative methods used in the fatigue crack growth calculations.

6.4.5 Summary of Fatigue Crack Growth Analysis

As shown in Table 6-10, for a partial through-wall crack in the RHR Line, the crack growth in the depth direction is 0.0014 inch and the crack growth in the length direction is 0.0004 inch. This is about 0.0009% of the 43.96 inch circumference length, and compared to the crack growth of 0.12% (12.50% to 12.62% in Table 4-1) in the depth direction, it is relatively small. For the Surge Line, the crack growth in the depth direction is 0.0855 inch and the crack growth in the length direction is 0.0452 inch. This is 0.113% of the 40.03 inch circumference length, and compared to the 7.6% (12.50% to 20.10% in Table 4-1) in the depth direction, it is relatively small. Overall, for the RHR and surge lines, the partial through-wall cracks tend to grow in the depth direction and through-wall before extending significantly in the length (circumferentially) direction. There is no growth in the accumulator line.

For through-wall flaws, as demonstrated in Table 6-11, crack growth of a postulated leakage flaw due to a conservative seismic event was insignificant and the final flaw size was smaller than the critical flaw size.

Table 6-1. Accumulator Line Operating Condition Transients

Transient	Design Transients	Occurrences(2)	$\Delta P^{(6)}$ (psi)	ΔT (°F)
1	Inadvertent RCS Depressurization	20(2)	1,117	490(3)
2	Inadvertent Accumulator Blowdown	4(4)	232	330(4)
3	Post LOCA Operation	1(4)	1,117	490(3)
4	OBE	50(7)		

Notes:
1. The above event counts reflect the 40-year design life, which is applicable to both 60 years and 80 years of operation per References [51] and [55].
2. Obtained from Reference [31].
3. Assumed as the temperature difference between typical cold leg temperature of 560°F and room temperature of 70°F.
4. Assumed based on similar plant design data [32, Table 4.3-2].
5. Assumed as the temperature difference between temperature of 400°F and room temperature of 70°F.
6. Conservatively calculated as the pressure difference between the saturated steam pressure at high temperature and ambient pressure.
7. Assumed the same as in Surge Line, obtained from Reference [50].

Table 6-2. RHR Line Operating Condition Transients [31]

Transient	Design Transients	Occurrences (2)	ΔP (psi)	ΔT (°F)
1	Heat Up /Cooldown	200 each	1925	437
2	Unit Load/Unload at 0-15% Full power	500 each	0(3)	9.6
3	Unit Load /Unload at 5% Full power	13,200	68(3)	55
4	Step Load Increase/Decrease of 10% Full power	2,000 each	109(3)	8.7
5	Reactor Trip with Cooldown and Safety Injection	10	539	139
6	Primary Side Leakage Test	200	800 (Assumed)	0 (Assumed)
7	OBE	50(4)		

Notes
1. Above transients are obtained from Reference [31].
2. The above event counts reflect the 40-year design life, which is applicable to both 60 years and 80 years of operation per References [51] and [55].
3. Conservatively assumed based on similar plant operational data.
2. Assumed the same as in Surge Line, obtained from Reference [50].

Table 6-3 Surge Line Operating Condition Transients [50]

Transient #	Design Transients	Occurrences(1)	Max Stress(3) (ksi)	Min Stress(3) (ksi)
1	Heatup	200(2)	10.158	-8.179
2	Unit Loading	13,200(2)	14.583	11.150
3	Step Load Increase and Decrease	4000	15.465	9.599
4	Large Step Load Decrease with Steam Dump	200	14.470	9.430
5	SS Fluctuation	3,150,000	12.232	10.895
6	Loss of Load	80	18.677	9.340
7	Loss of Power	40	17.259	9.449
8	Loss of Flow	80	14.286	9.299
9	Reactor Trip	400	15.963	2.654
10	Inadvertent Auxiliary Spray	10	15.045	11.108
11	OBE	50	15.735	3.972
12	Unit Unloading	13,200(2)	14.583	11.150
13	Cool Down	200(2)	10.158	-8.179
14	Turbine Roll Test	10	2.292	0.000
15	Hydrotest @3107 psi	5	9.858	0.000
16	Leak Test @ 2485 psi	50	8.145	0.000

Notes
1. The above event counts reflect the 40-year design life, which is applicable to both 60 years and 80 years of operation per References [51] and [55].
2. Obtained from Reference [31].
3. Values are assumed the same as unit loading transient.

Table 6-4. Piping Loads for Accumulator and RHR Lines

Components	Deadweight Moments (ft-lb)			Thermal Moments (ft-lb)			OBE Moments (ft-lb)		
	Mx	My	Mz	Mx	My	Mz	Mx	My	Mz
Accumulator Lines	2,847	5,545	25,236	38,919	33,733	26,644	40,607	38,813	17,688
RHR Lines	3,574	2,721	15,696	96,351	88,786	66,018	35,002	52,858	23,458

Table 6-5. Accumulator Line Maximum and Minimum Transient Stresses

Transient	Maximum Stresses (ksi)				Minimum Stresses (ksi)			
	Pressure	Thermal	DW	Total	Pressure	Thermal	DW	Total
1	2.193	10.169	0.000	0.000	22.838	2.193	33.007	0.000
2	2.648	17.017	1.737	3.320	22.838	2.648	39.856	1.737
3	4.386	20.338	0.000	0.000	22.838	4.386	43.176	0.000
4	4.878	0.000	4.558	19.764(1)	4.878	0.000	4.558	-0.891(1)

Note: (1) The OBE stress (10.32 ksi) is added to maximum stress and subtracted from minimum stress.

Table 6-6. RHR Line Maximum and Minimum Transient Stresses

Transient	Maximum Stresses (ksi)				Minimum Stresses (ksi)			
	Pressure	Thermal	DW	Total	Pressure	Thermal	DW	Total
1	3.993	10.810	1.335	16.139	0.000	0.000	1.335	1.335
2	3.993	11.048	1.335	16.376	3.993	10.573	1.335	15.901
3	4.134	12.171	1.335	17.640	3.852	9.450	1.335	14.637
4	4.220	11.025	1.335	16.580	3.767	10.595	1.335	15.697
5	5.112	14.249	1.335	20.695	2.875	7.372	1.335	11.582
6	5.653	10.810	1.335	17.798	2.334	10.810	1.335	14.479
7	4.637	0	1.335	11.499(1)	4.637	0.000	1.335	0.444(1)

Note: (1) The OBE stress (5.53 ksi) is added to maximum stress and subtracted from minimum stress.

Table 6-7. Stress Range for Accumulator Line

Group	Cyclic Stresses (ksi)				DW + Residual (ksi)	Total Stress Ranges (ksi)			
	Maximum		Minimum			Maximum		Minimum	
	Uniform	Linear	Uniform	Linear		Uniform	Linear	Uniform	Linear
1	2.193	10.169	0.000	0.000	22.838	2.193	33.007	0.000	22.838
2	2.648	17.017	1.737	3.320	22.838	2.648	39.856	1.737	26.159
3	4.386	20.338	0.000	0.000	22.838	4.386	43.176	0.000	22.838
4	4.878	10.328	4.878	-10.328	22.838	4.878	33.166	4.878	12.511

Table 6-8. Stress Range for RHR Line

Group	Cyclic Stresses (ksi)				DW +Residual(ksi)	Total Stress Ranges (ksi)			
	Maximum		Minimum			Maximum		Minimum	
	Uniform	Linear	Uniform	Linear		Uniform	Linear	Uniform	Linear
1	3.993	10.810	0.000	0.000	19.615	3.993	30.425	0.000	19.615
2	3.993	11.048	3.993	10.573	19.615	3.993	30.663	3.993	30.188
3	4.134	12.171	3.852	9.450	19.615	4.134	31.786	3.852	29.065
4	4.220	11.025	3.767	10.595	19.615	4.220	30.641	3.767	30.210
5	5.112	14.249	2.875	7.372	19.615	5.112	33.864	2.875	26.987
6	5.653	10.810	2.334	10.810	19.615	5.653	30.425	2.334	30.425
7	4.637	5.528	4.637	-5.528	19.615	4.6365	25.143	4.637	14.087

Table 6-9. Stress Range for Surge Line

Transient #	Total Stress Ranges (ksi)			
	Maximum(1)		Minimum	
	Uniform	Linear	Uniform	Linear
1	4.742	23.696	0.000	10.101
2	4.742	28.121	0.000	29.430
3	4.742	29.003	0.000	27.879
4	4.742	28.008	0.000	27.710
5	4.784(2)	25.728	4.700(2)	24.475
6	4.742	32.215	0.000	27.620
7	4.742	30.797	0.000	27.729
8	4.742	27.824	0.000	27.579
9	4.742	29.501	0.000	20.934
10	4.742	28.583	0.000	29.388
11	4.742	29.273	0.000	22.252
12	4.742	28.121	0.000	29.430
13	4.742	23.696	0.000	10.101
14	4.742	15.830	0.000	18.280
15	6.548(3)	21.590	0.000	18.280
16	5.237(4)	21.188	0.000	18.280

Note:
(1) For all the transients with no pressure information, the operating pressure of 2250 psi is conservatively used to calculate the Maximum uniform stress.
(2) For Transient 5 (steady state fluctuation as shown in Table 6-3), a typical pressure ±20psi was added to 2,250 to calculate the maximum and minimum uniform stress
(3) The pressure of 3,107psi, as shown in Table 6-3, is used.
(4) The pressure of 2,485 psi, as shown in Table 6-3, is used.

Table 6-10. Results of Fatigue Crack Growth Analysis for Part Through-Wall Flaws

Auxiliary Lines	**Postulated Initial Flaw**			**60 Years (ASME Section XI)**			**80 Years (ASME CC N-809)**		
	a/t	**Depth a_i (in)**	**Half Length c_i (in)**	**a/t**	**Depth a_f (in)**	**Half Length c_f (in)**	**a/t**	**Depth a_f (in)**	**Half Length c_f (in)**
Accumulator Line	12.50%	0.1250	0.6250	12.50%	0.1250	0.6250	12.50%	0.1250	0.6250
RHR Line	12.50%	0.1563	0.7815	12.50%	0.1563	0.7815	12.62%	0.1577	0.7817
Surge Line	12.50%	0.1406	0.7030	12.57%	0.1414	0.7031	20.10%	0.2261	0.7256

Table 6-11. Results of Fatigue Crack Growth Analysis for Through-Wall Flaws

Auxiliary Line	Postulated Initial Leakage Flaw	60 Years (ASME Section XI)	80 Years (ASME CC N-809)	Critical Flaw Size
	Half Length a_L (in)	Half Length a_f (in)	Half Length a_f (in)	Half Length a_c (in)
Accumulator Line	2.53	2.622	2.760	4.61
RHR Line	3.12	3.203	3.334	6.35
Surge Line	3.30	3.409	3.558	4.06

7.0 CONCLUSIONS

Leak-before-break (LBB) evaluations are performed for RCS auxiliary piping at PTN Units 3 and 4 in accordance with the requirements of NUREG-1061. The evaluation included the following lines:

1. 10" diameter Accumulator Lines – 3 lines (one per RCL connected to cold leg)
2. 12" pressurizer Surge Line – 1 line attached to "B" loop
3. 14" residual heat removal line – 1 line attached to "C" loop in Unit 3 and "A" loop in Unit 4 (connected to hot leg)

The approach taken herein is consistent with SRP 3.6.3 and has been used in recent LBB submittals for other plants [2, 3, 4]. The analysis was performed using conservative lower bound material properties for the base metals and weldments and location specific stresses consisting of pressure, deadweight, thermal and SSE loads. The evaluations considered only circumferential flaws since previous evaluations have shown them to be more limiting than axial flaws. Critical flaw sizes and leakage flaw sizes were calculated on a location specific basis using limit load analysis. The leakage flaw size is defined as the minimum of one half the critical flaw size with a factor of one on the stresses. Leakage was then calculated through the leakage flaw size. Bounding analysis curves (BAC) were then derived which provide loci of acceptable normal operating loads (for leakage calculation) and normal +SSE loads (for critical flaw size calculation) for a given leakage. Fatigue crack growth analysis was also performed to determine the extent of growth of any pre-existing flaws.

Based on these evaluations, the following conclusions can be made.

- For both PTN Units 3 and 4, all of the stress points of the 5 analyzed lines are under or very close to the BACs of 10 GPM leakage, which correspond to the 1 GPM detection capability.
- Fatigue crack growth of an assumed surface flaw is less than ASME Code Section XI allowable flaw size for the most limiting locations for all piping under consideration in this evaluation. In addition, crack growth of a postulated leakage flaw due to a conservative seismic

event was insignificant and the final flaw size was smaller than the critical flaw size. This demonstrates that a leakage flaw will remain stable during an SSE event.

- The effect of degradation mechanisms that could invalidate the LBB evaluations was considered in the evaluation. A determination was made that there is no potential for water hammer, intergranular stress corrosion cracking (IGSCC) and erosion-corrosion for the piping systems considered in the LBB evaluations.

In conclusion, the five auxiliary lines of the RCL piping systems of PTN Units 3 and 4 evaluated in this report qualify for the application of leak-before-break analysis to demonstrate that it is very unlikely that the piping could experience a large pipe break prior to leakage detection.

8.0 REFERENCES

1. EPU Bechtel/Engineering Services Project Scope Document, "Development of Technical Report to Apply Leak-Before-Break (LBB) Methodology to Auxiliary Lines Connected to Primary Reactor Coolant Loops at Turkey Point Units 3 and 4".

2. Letter from G. S. Vissing (USNRC) to R. C. McCredy (RG&E) including Safety Evaluation Report, "Staff Review of the Submittal by Rochester Gas & Electric to Apply Leak Before Break Status to portions of R. E. Ginna Nuclear Power Plant Residual Heat Removal System Piping (TAC No. MA039)", dated February 25, 1999, Docket No. 50-244.

3. Letter from R. B. Eaton (USNRC) to R. P. Necci (Northeast Nuclear Energy Company) including Safety Evaluation Report, "Staff Review of the Submittal by Northeast Nuclear Energy Company to Apply Leak Before Break Status to the Pressurizer Surge Line, Millstone Nuclear Power Station Unit 2 (TAC No. MA4146)", dated May 4, 1999, Docket No. 50-336.

4. Letter from J. G. Lamb (USNRC) to T. Contu (Nuclear Management Company, LLC) including Safety Evaluation Report, "Kewaunee Nuclear Power Plant - Review of the Leak Before Break Evaluation for the Residual Heat Removal, Accumulator Injection Line, and Safety Injection System (TAC No. MB1301)", dated September 5, 2002, Docket No. 50-305.

5. Stello, Jr., V., "Final Broad Scope Rule to Modify General Design Criterion 4 of Appendix A, 10 CFR Part 50," NRC SECY-87-213, Rulemaking Issue (Affirmation), August 21, 1987.

6. NUREG-1061, Volumes 1-5, "Report of the U. S. Nuclear Regulatory Commission Piping Review Committee," prepared by the Piping Review Committee, NRC, April 1985.

7. NUREG-0800, Revision 1, "U.S. Nuclear Regulatory Commission Standard Revision Plan, Office of Nuclear Reactor Regulation, Section 3.6.3, Leak-Before-Break Evaluation Procedure," March 2007.

8. FPL Document, " Leak Detection Capabilities 3/4.4.6," SI File 0901350.206.

9. NUREG-0927, "Evaluation of Water Hammer Occurrence in Nuclear Power Plants," Revision 1.

10. W. S. Hazelton and W. H. Koo, "Technical Report on Material Selection and Processing Guidelines for BWR Coolant Pressure Boundary Piping," NUREG-0313, Rev. 2, USNRC, January 1988.

11. EPRI Report No. NP-3944, "Erosion/Corrosion in Nuclear Power Plant Steam Piping: Causes and Inspection Program Guidelines," April 1985

12. NRC Bulletin No. 88-08, "Thermal Stresses in Piping Connected to Reactor Coolant Systems," June 22, 1988.

13. FPL Stress Report SP-13, 14, 15 (TR 5322-43) "Unit 3 Book 1 of 16-Technical Report".

14. FPL Stress Report SP-13, 14, 15 SP-044 (TR-5322-126), "Unit 4 book 1 of 7-Technical Report".

15. Crane Co., Technical Paper No. 410, "Flow of Fluid Through Valves, Fittings, and Pipe", 1976.

16. FPL Stress Report SP-041 (TR-5322-135), "Units 3 and 4 Book 1 of 4 Technical Report".

17. FPL Drawing 5613-P-766, Sheet 1 of 3, Rev. 5, "Turkey Point Nuclear Power Plant Unit 3".

18. FPL Drawing 5614-P-766, Sheet 1 of 3, Rev. 3, "Turkey Point Nuclear Power Plant Unit 4".

19. FPL Technical Report SI-13 TR-5322-15, Rev. 1, "Unit 3-RHR System".

20. FPL Technical Report SI-16 TR-5322-155, Rev. 1, "Unit 4 Book 1 Report and Book 2-BPC Stress Run".

21. FPL Document MN-3.11, "Piping Specification".

22. Bechtel Document P8-AT-AG, "Bechtel Welding Procedure Qualification Record PQR No. 47".

23. FPL Drawing 40038, Rev. 2, "10″ Sch. 140 BW. Nozzle Reactor Coolant Piping".

24. FPL Document WPS-43, Sheet 2 of 3, Rev. 11, "Welding Procedure Specification".

25. ASME Boiler and Pressure Vessel Code, Section II, Part D - Properties, 2001 Edition with Addenda through 2003.

26. ASME Boiler and Pressure Vessel Code, Section XI, 2001 Edition with Addenda through 2003.

27. EPRI Report No. NP-5531, "Evaluation of High-Energy Pipe Rupture Experiments," January 1988.

28. EPRI Report NP-3596-SR, "PICEP: Pipe Crack Evaluation Computer Program," Rev. 1, July 1987.

29. P.E. Henry, "The Two-Phase Critical Discharge of Initially Saturated or Sub-cooled Liquid," Nuclear Science and Engineering, Vol. 41, 1970.

30. EPRI Report NP-3395, "Calculation of Leak Rates Through Crack in Pipes and Tubes," December 1983.

31. Material Reliability Program: Characterization of U.S. Pressurized Water Reactor (PWR) Fleet Operational Transients (MRP-393), EPRI, Palo Alto, CA; 2014, 3002003085.

32. License Renewal Application, Callaway Plant, Unit 1, Facility Operating License No. NPF-30. http://www.nrc.gov/reactors/operating/licensing/renewal/applications/callaway.html

33. Section XI Task Group for Piping Flaw Evaluation, ASME Code, "Evaluation of Flaws in Austenitic Steel Piping, " Journal of Pressure Vessel Technology, Vol. 108, August 1986.

34. FPL Drawing 5613-P-585, Sheet 1 of 1, Rev. 6, "Turkey Point Nuclear Power Plant Unit 3".

35. FPL Drawing 5613-P-586, Sheet 1 of 1, Rev. 6, "Turkey Point Nuclear Power Plant Unit 3".

36. FPL Drawing 5613-P-587, Sheet 2 of 2, Rev. 4, "Turkey Point Nuclear Power Plant Unit 3".

37. FPL Drawing 5613-P-669, Sheet 1 of 1, Rev. 5, "Turkey Point Nuclear Power Plant Unit 3".

38. FPL Drawing 5613-P-766, Sheet 2 of 3, Rev. 4, "Turkey Point Nuclear Power Plant Unit 3".

39. FPL Drawing 5614-P-509, Sheet 1 of 4, Rev. 9, "Turkey Point Nuclear Power Plant Unit 4".

40. FPL Drawing 5614-P-509, Sheet 3 of 4, Rev. 3, "Turkey Point Nuclear Power Plant Unit 4".

41. FPL Drawing 5614-P-509, Sheet 4 of 4, Rev. 3, "Turkey Point Nuclear Power Plant Unit 4".

42. FPL Drawing 5614-P-574, Sheet 1, Rev. 5, "Turkey Point Nuclear Power Plant Unit 4".

43. FPL Drawing 5614-P-766, Sheet 2 of 3, Rev. 2, "Turkey Point Nuclear Power Plant Unit 4".

44. (a) FPL Stress Report SP-13, 14, 15 (TR 5322-43) "Unit 3 Book 6 of 16-BPC Stress Run".

    (b) FPL Stress Report SP-13, 14, 15 (TR 5322-43) "Unit 3 Book 7 of 16- BPC Stress Run".

    (c) FPL Stress Report SP-13, 14, 15 (TR 5322-43) "Unit 3 Book 8 of 16- BPC Stress Run".

    (d) FPL Stress Report SP-13, 14, 15 (TR 5322-43) "Unit 3 Book 9 of 16- BPC Stress Run".

    (e) FPL Stress Report SP-13, 14, 15 (TR 5322-43) "Unit 3 Book 8 of 16- BPC Stress Run".

    (f) FPL Stress Report SP-13, 14, 15 (TR 5322-43) "Unit 3 Book 9 of 16- BPC Stress Run".

45. (a) FPL Stress Report SP-044 (TR 5322-126) "Unit 4 Book 6 of 7- BPC Stress Run".

    (b) FPL Stress Report SP-044 (TR 5322-126) "Unit 4 Book 7 of 7- BPC Stress Run".

46. FPL Stress Report SP-041 (Stress Problem 041), "FPL/FLA (Turkey point 3 and 4) Pressurizer Surge Nozzle Fatigue Calculations Due to Thermal Stratification Piping Loads – NRC Review".

47. FPL Stress Report SI-13 (TR 5322-15) "Unit 3 Book 2 of 2- BPC Stress Run."

48. FPL Stress Report SI-16 (TR 5322-155) "Unit 4 Book 2 of 2- BPC Stress Run."

49. **pc-CRACK**.
    a. **pc-CRACK** 4.1 CS, Version Control No. 4.1.0.0, Structural Integrity Associates, December 31, 2013.
    b. **pc-CRACK 4.2**, Version Control No. 4.2.0.0, Structural Integrity Associates, April 2018.

50. FPL Stress Report (TR 0537), "FPL/FLA (Turkey Point 3 and 4) Pressurizer Surge Nozzle Fatigue Calculation Due to Thermal Stratification Pipe Loads".

51. SI Report No. 1700109.402P, Revision 4, "*Evaluation of Fatigue of ASME Section III, Class 1 Components for Turkey Point Units 3 and 4 for Subsequent License Renewal*".

52. FPL Document EPU-PTN-10-0536, "FPL TURKEY POINT UNITS 3 & 4 EXTENDED POWER UPRATE (EPU) INFORMATION FOR LEAK BEFORE BREAK METHODOLOGY APPLIED TO RCL BRANCH PIPING".

53. ASME Code Case N-809, "Reference Fatigue Crack Growth Rate Curves for Austenitic Stainless Steels in Pressurized Water Reactor Environments Section XI, Division 1," Cases of the ASME Boiler and Pressure Vessel Code, June 23, 2015.

54. SI Corrective Action Report (CAR) No. 17-012, Revision 0, "Turkey Point LBB Evaluation, Calculation Package File No.: 0901350.304, Rev. 0, Calculation Title: Fatigue Crack Growth Evaluation," April 17, 2017.

55. Turkey Point Units 3 and 4 License Renewal Document, "Position Document to Address GSI-190 Issues Related to Fatigue Evaluation for Turkey Point Units 3 and 4", SI Report No. SIR-00-089. Rev. 0.